Radiation In-Port Cross-Talks of ITER Port Diagnostics

A. Serikov[1], U. Fischer[1], D. Anthoine[2], L. Bertalot[3], M. De Bock[3], R. O'Connor[3], R. Juarez[4], V. Krasilnikov[3]

[1]Karlsruhe Institute of Technology (KIT), Institute for Neutron Physics and Reactor Technology, Hermann-von-Helmholtz-Platz 1, 76344 Eggenstein-Leopoldshafen, Germany
[2]Bertin Technologies, France
[3]ITER Organization, Route de Vinon-sur-Verdon, CS 90 046, 13067 St. Paul Lez Durance Cedex, France
[4]Departamento de Ingeniería Energética, ETSII-UNED, Calle Juan del Rosal 12, Madrid 28040, Spain

Email corresponding author: arkady.serikov@kit.edu

Content

- **Objectives** (phenomenon of radiation cross-talks between Diagnostic systems)
- **Examples of in-port cross-talks:**

  1) Tritium and Deposition Monitor (TDM) & CIXS in Local model of **EPP #17**

  2) Tangential Neutron Spectrometer (TNS) inside the **EPP #8** with 7 Diagnostics in C-lite v.2

  3) Shutter and the main Diagnostic path of the Charge eXchange Recombination Spectroscopy (CXRS) in **UPP #3**
- **Conclusions**

Example 1: Tritium and Deposition Monitor (TDM) & CIXS in Local model of **EPP #17**

MCNP Local modeling approach and mesh-tallies

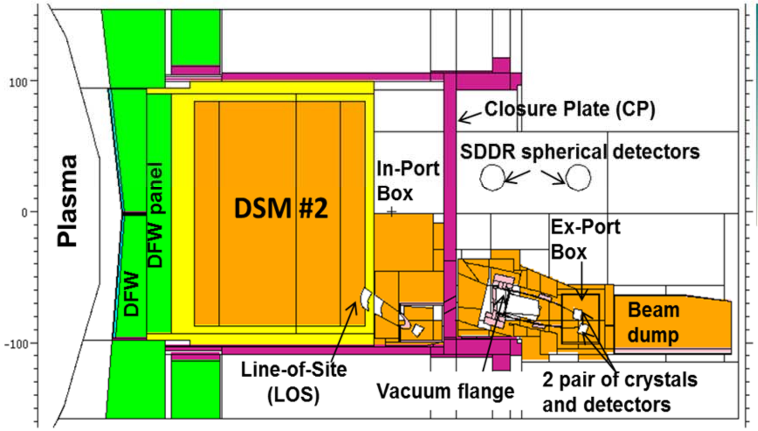

Initial MCNP local model of the **CIXS** Diagnostics apertures only

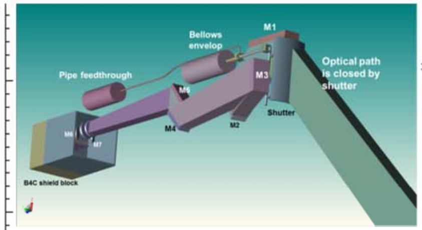

Converted CAD-to-MCNP T-monitor model is inserted in EPP17 MCNP Local model

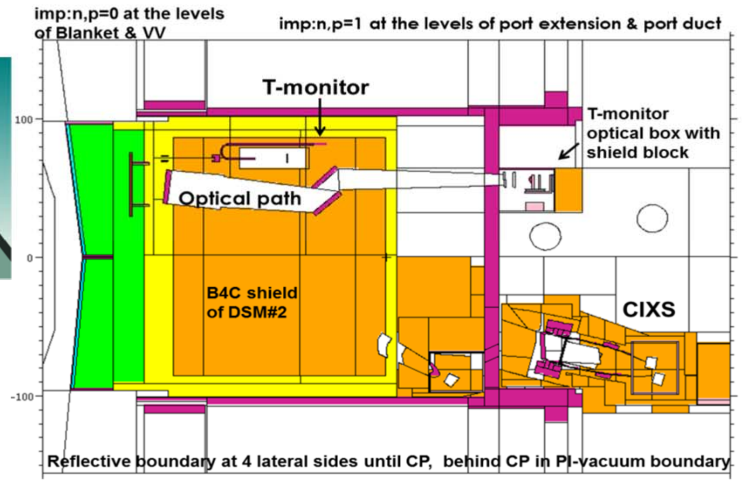

Resulting MCNP local model with Diagnostics apertures of two systems: **Tritium (T) monitor & CIXS**

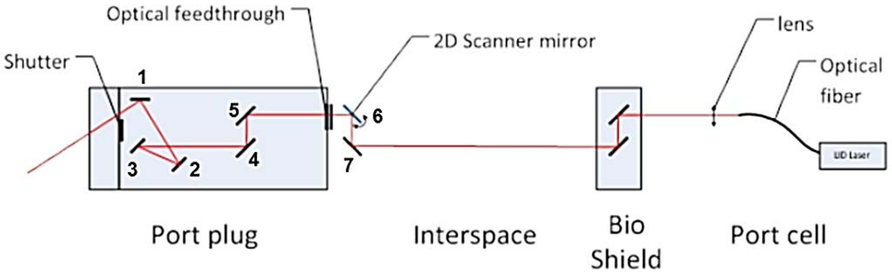

7 mirrors M1-M7 have been modelled - along the optical pathway, started from the front mirror M1, ended by M7 inside the optical box attached to the Closure Plate

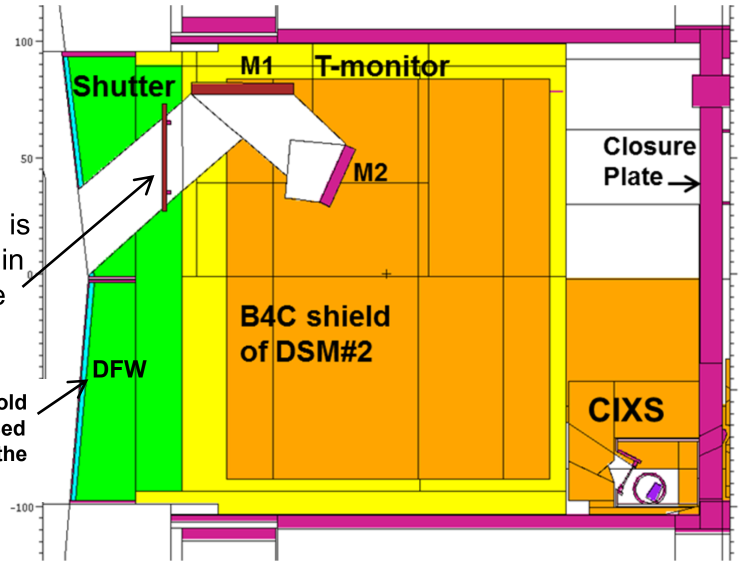

Optical path is closed by thin shutter plate

DFW "V" shape is the old version but we supposed this has no impact on the presented results

Total neutron flux for EPP17 with CIXS only

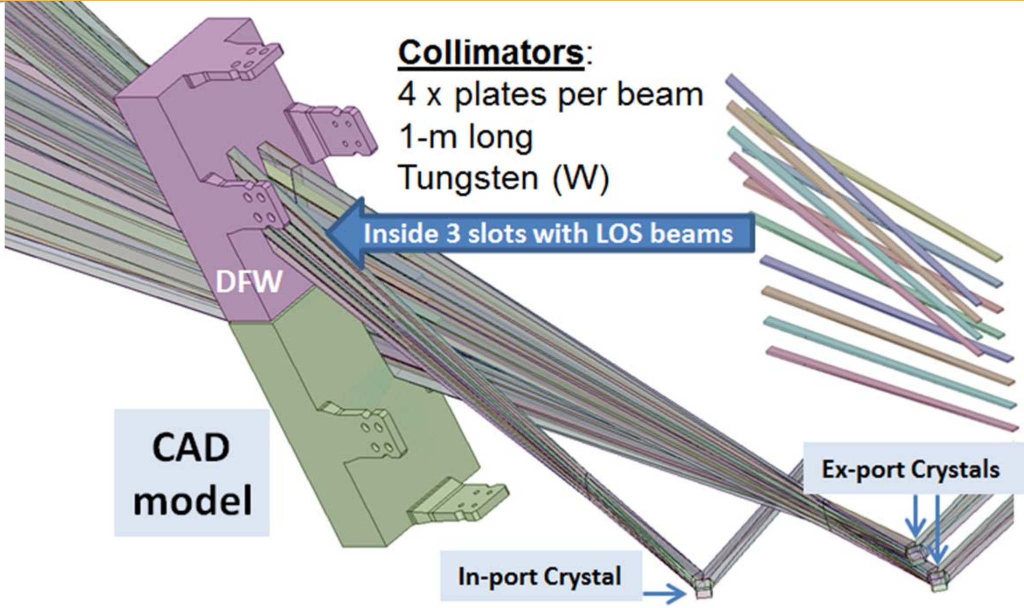

CAD model of the original CIXS shielding

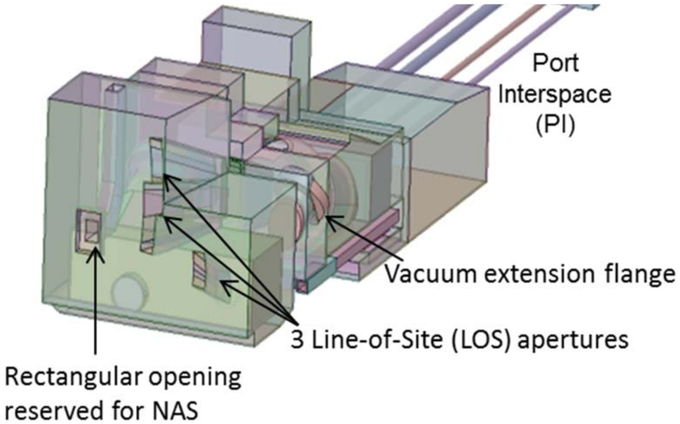

Map of total n-flux for the CIXS model having no-collimated LOS beams

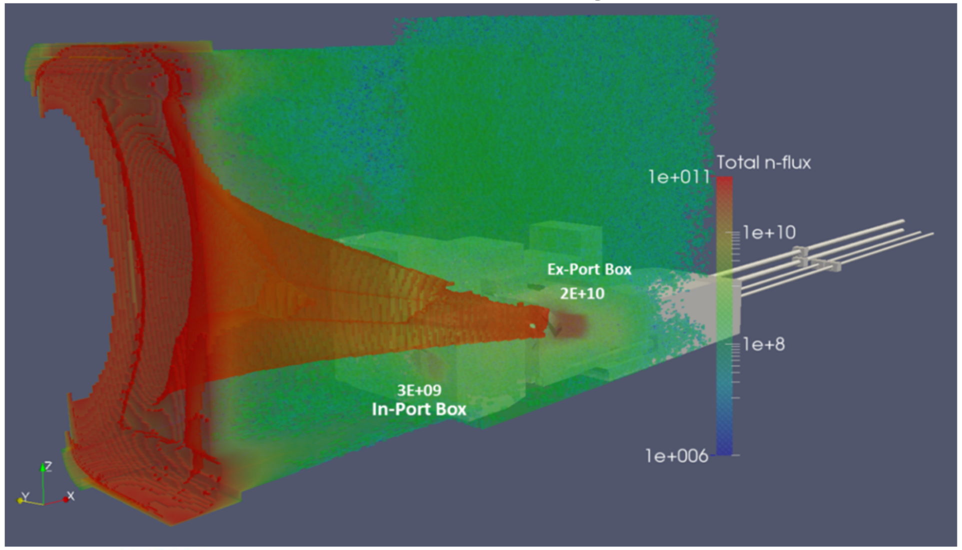

Map of total n-flux for the CIXS model with collimated LOS beams

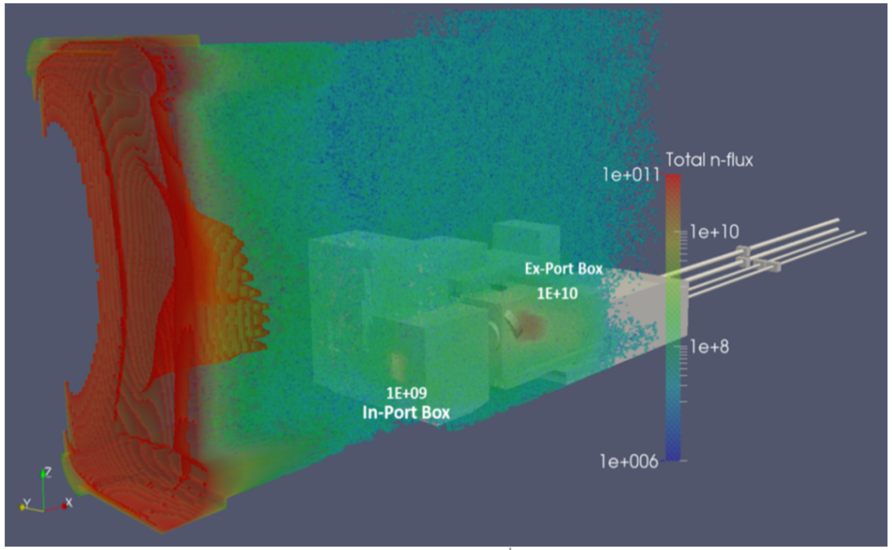

Total neutron flux for EPP17 with CIXS and TD-monitor

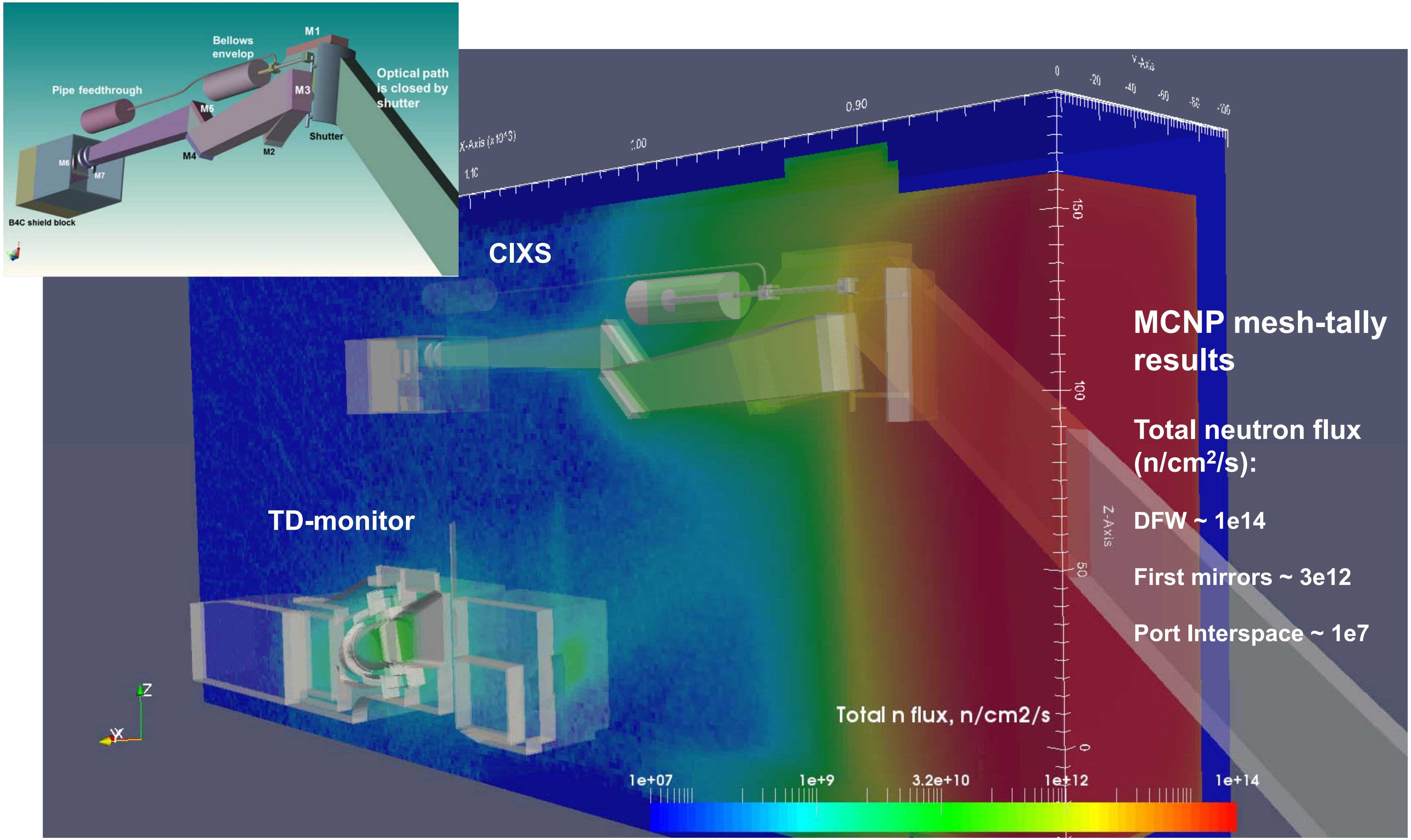

MCNP mesh-tally results

Total neutron flux ($n/cm^2/s$):

DFW ~ 1e14

First mirrors ~ 3e12

Port Interspace ~ 1e7

Too small vertical shift in a bend segment M4-M5

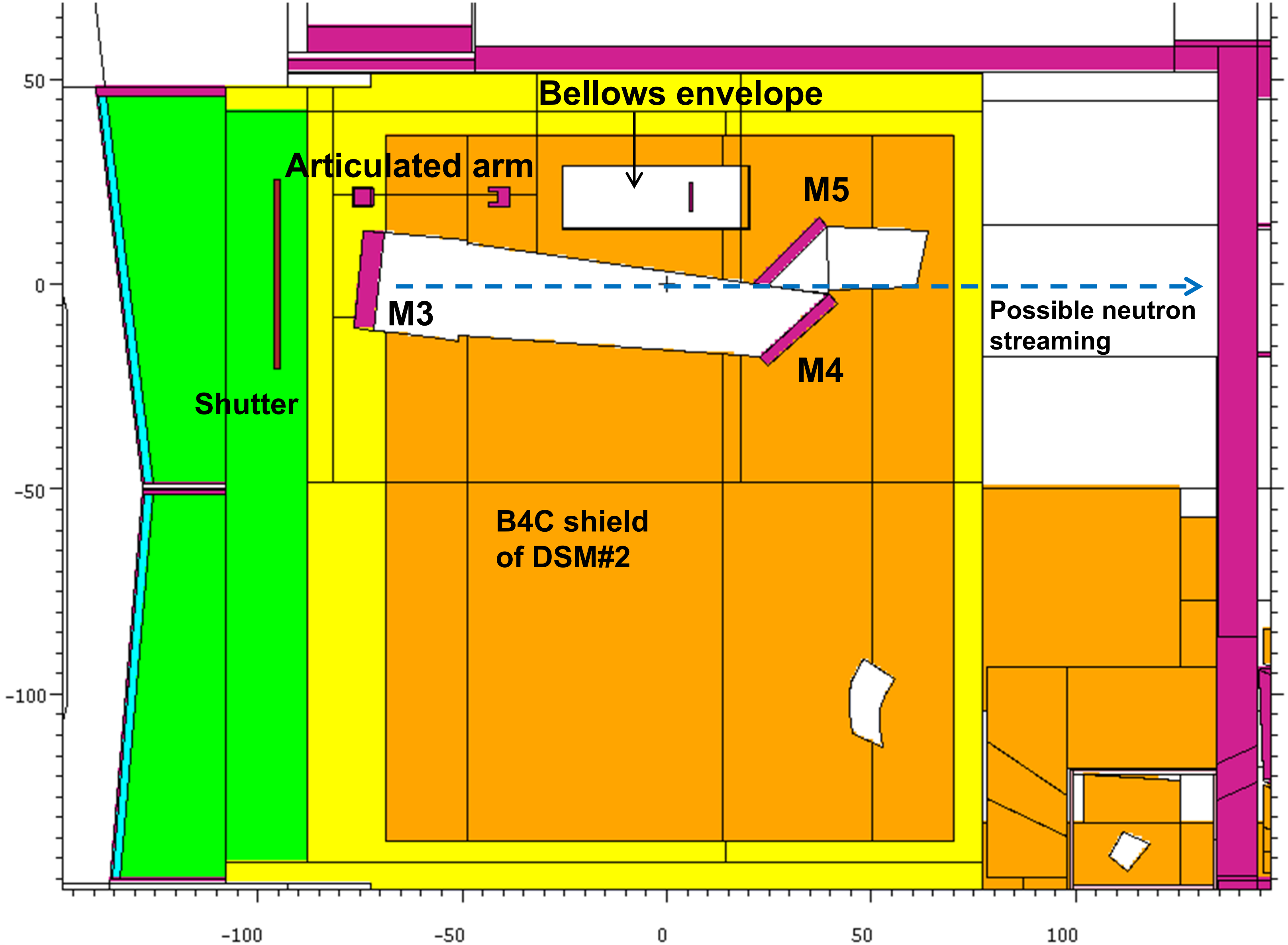

Neutron and gamma loads on the TD-monitor mirrors

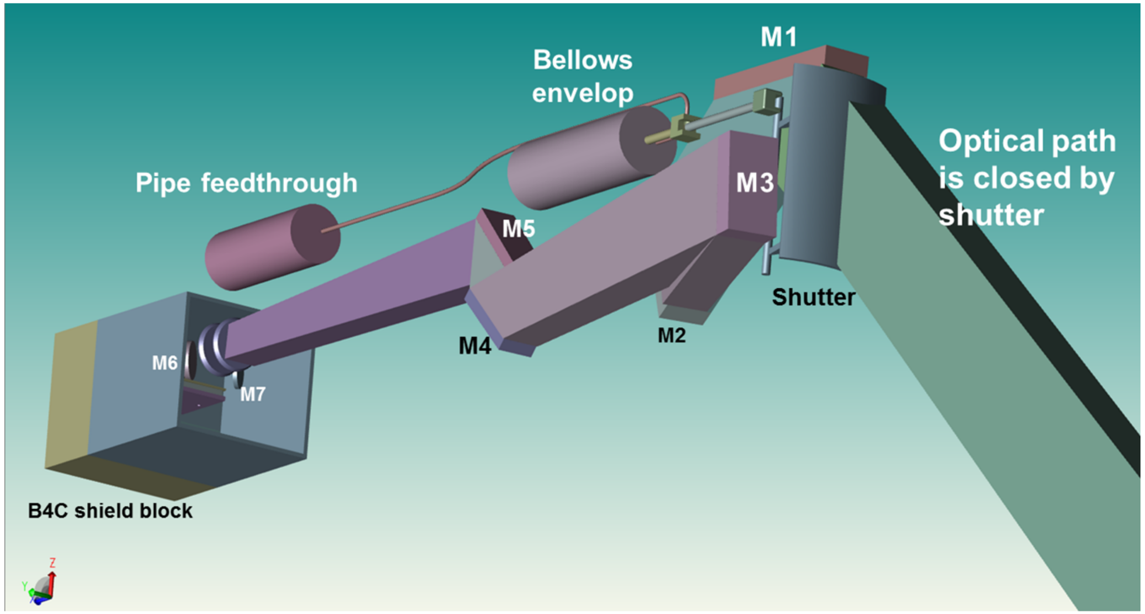

Neutron loads on mirrors

Mirror number	Neutron flux E<0.1 MeV, n/cm2/s	Neutron flux E>0.1 MeV, n/cm2/s	Total neutron flux, n/cm2/s
M1	1.26E+12	1.88E+12	3.14E+12
M2	1.36E+11	1.86E+11	3.22E+11
M3	1.77E+12	1.75E+12	3.51E+12
M4	9.52E+09	1.57E+10	2.52E+10
M5	2.23E+09	3.62E+09	5.85E+09
M6	8.48E+07	1.62E+08	2.47E+08
M7	2.66E+07	3.41E+07	6.07E+07

Fast neutrons (E>0.1 MeV), except of M3, dominate in total neutron fluxes on the mirrors.
Gamma deposition defines the total heat.
All the results are averaged over the mirror volumes.

Summary table of the neutronic loads on mirrors – fluxes and nuclear heat averaged over the mirror volumes

MCNP cell number	Mirror number	Material	Volume, cm3	Total neutron flux, n/cm2/s	Total gamma flux, gamma/ cm2/s	Neutron heating, W/cm3	Gamma heating, W/cm3	Total (n + gamma) heating, W/cm3
Cell 18554	M1	Molybdenum (Mo)	2640.81	3.14E+12	1.29E+12	3.11E-02	7.42E-01	7.73E-01
Cell 18555	M2	St. steel (SS316L(N)-IG)	1485.23	3.22E+11	1.48E+11	2.98E-03	3.87E-02	4.17E-02
Cell 18618	M3	St. steel (SS316L(N)-IG)	1360.83	3.51E+12	8.54E+11	2.21E-02	2.88E-01	3.10E-01
Cell 18556	M4	St. steel (SS316L(N)-IG)	601.99	2.52E+10	1.39E+10	3.48E-04	3.99E-03	4.34E-03
Cell 18559	M5	St. steel (SS316L(N)-IG)	567.48	5.85E+09	5.31E+09	8.50E-05	1.63E-03	1.71E-03
Cell 18557	M6	St. steel (SS316L(N)-IG)	85.49	2.47E+08	9.25E+07	4.24E-06	4.18E-05	4.60E-05
Cell 18558	M7	St. steel (SS316L(N)-IG)	50.33	6.07E+07	1.44E+07	8.97E-07	4.75E-06	5.65E-06

For all the presented results in mirrors, the statistical uncertainty expressed in Monte Carlo MCNP relative errors are less then 1% for the mirrors M1-M5, and around 10% for the mirrors M6-M7 behind the Closure Plate.

Distribution of decay gamma sources for SDDR

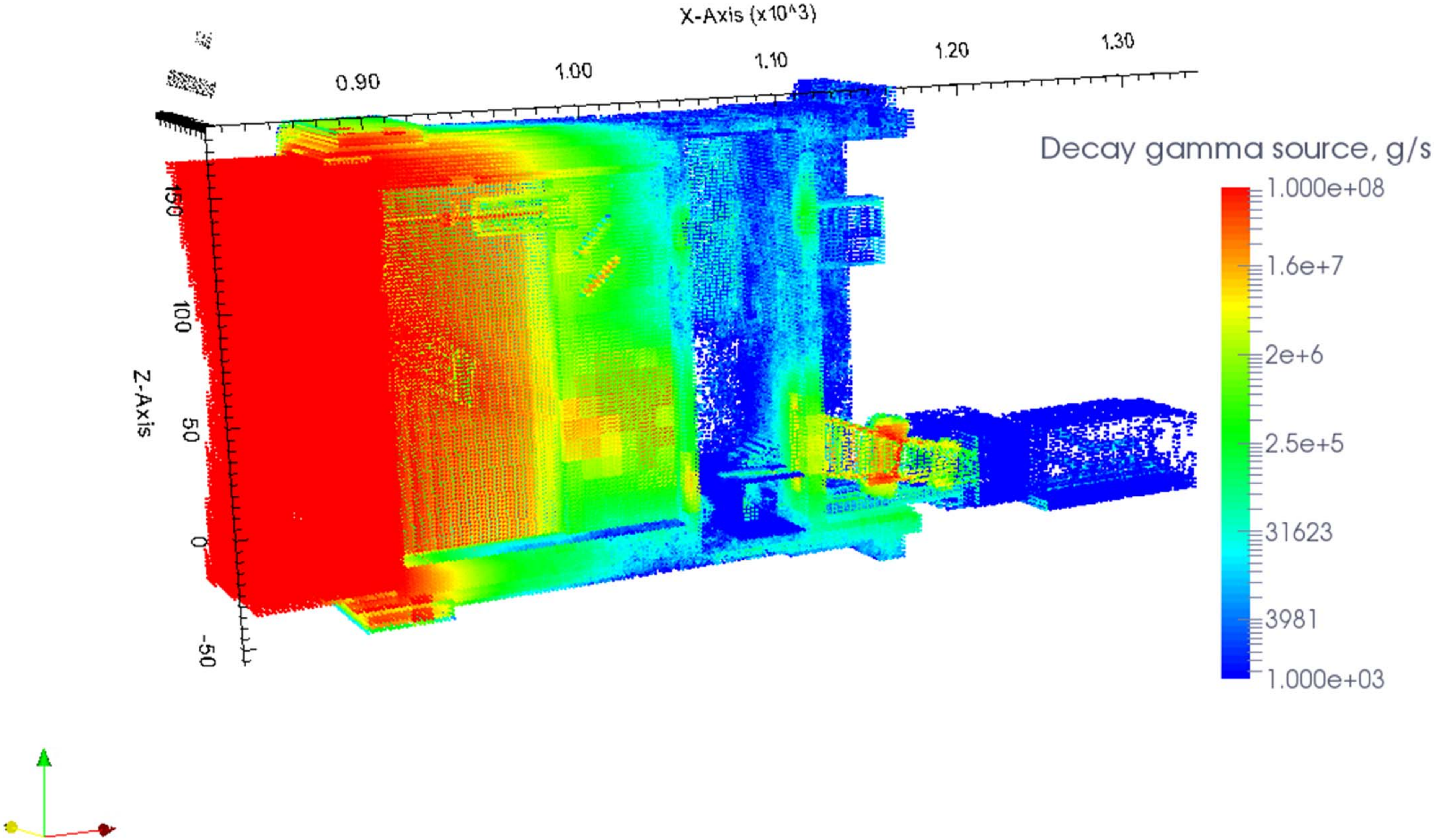

SDDR (Sv/h) map thresholded between **300 microSv/h** (at contact with flange) and **50 microSv/h** (dose level of maintenance access) – radial extent (X-axis) for CIXS without shield

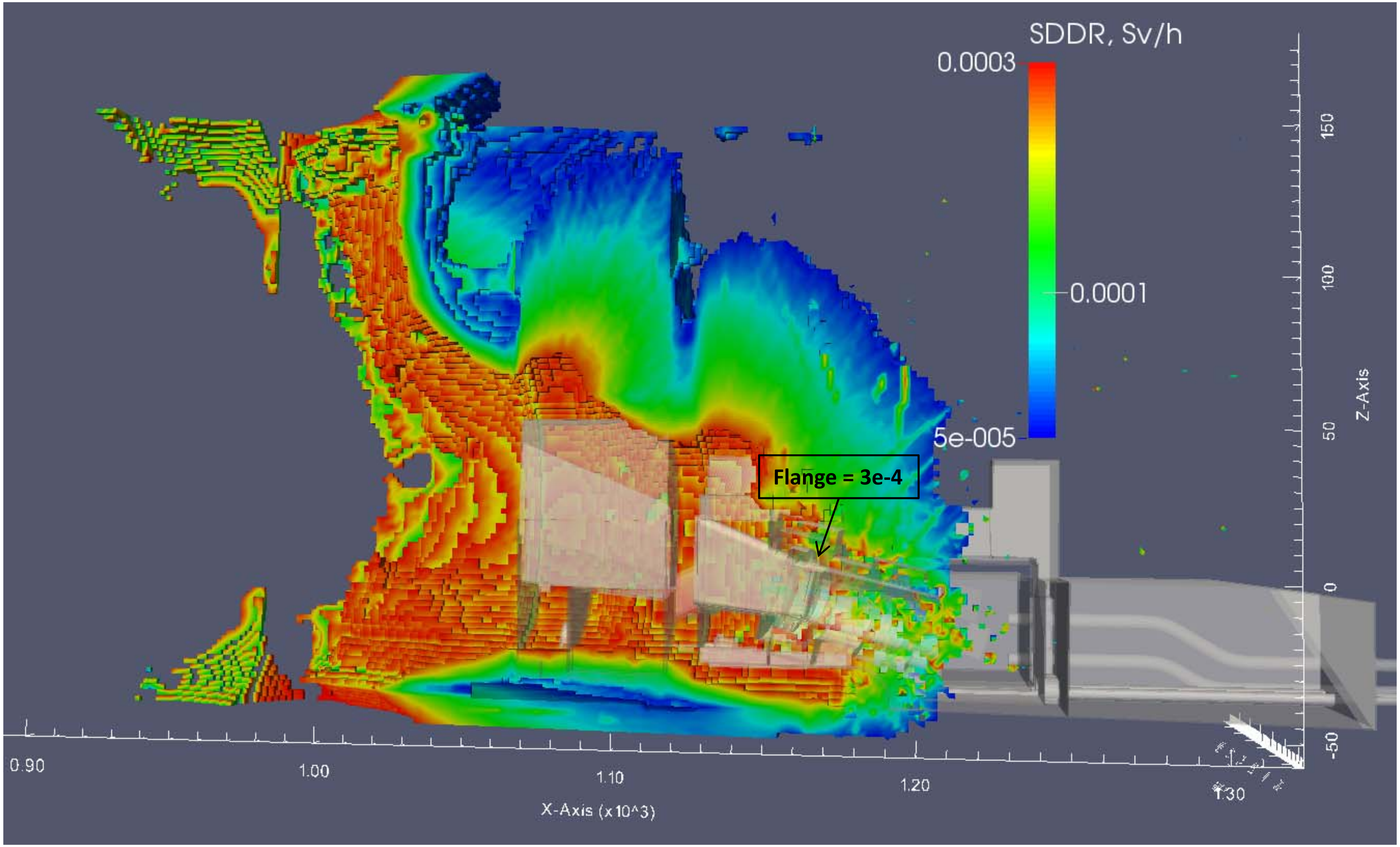

Axis coordinates in **cm**

SDDR for EPP17 with 2 diagnostics systems integrated: TD-monitor and CIXS

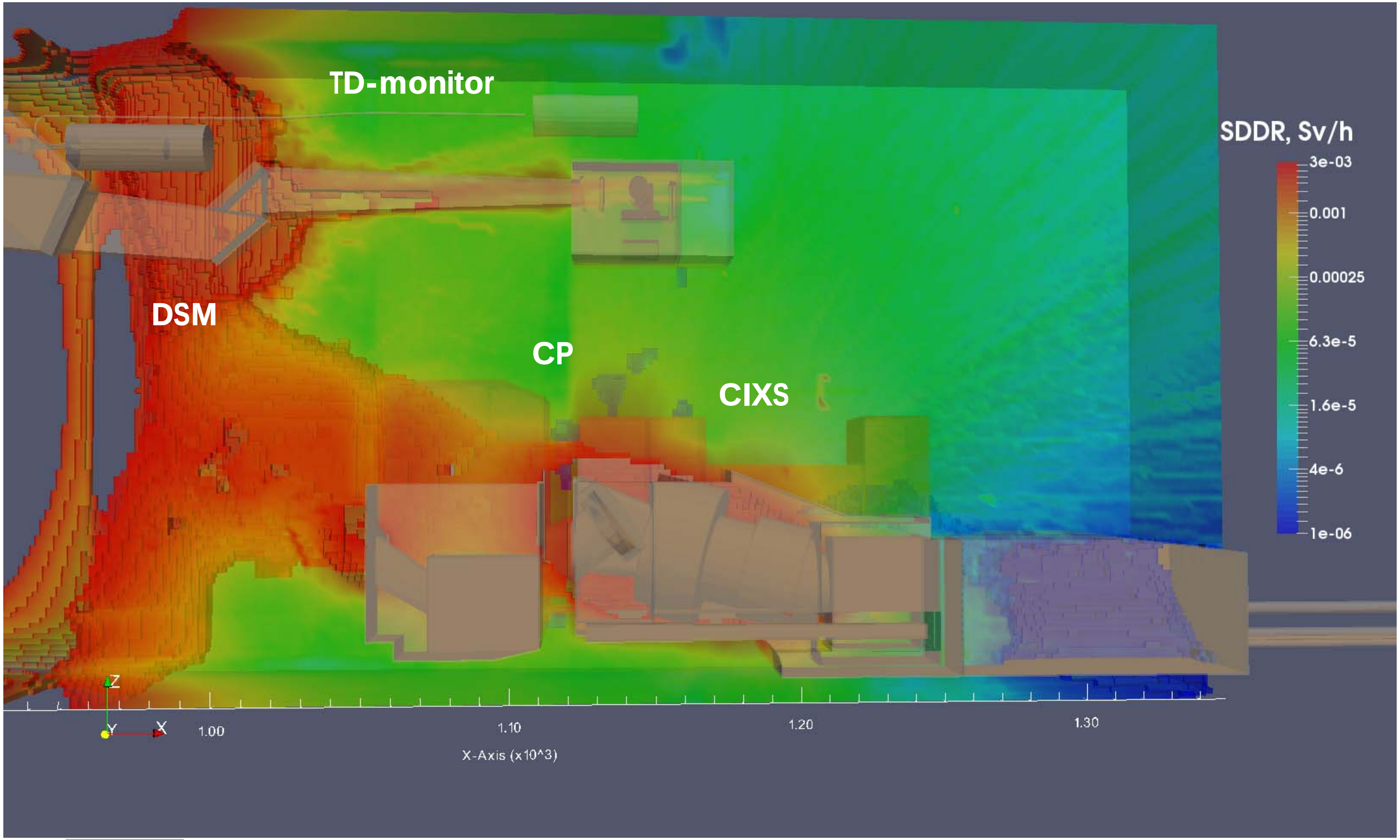

Comparison of the SDDR distributions in MCNP fine mesh

SDDR in CIXS-only model vs. **SDDR in TD-monitor & CIXS model**

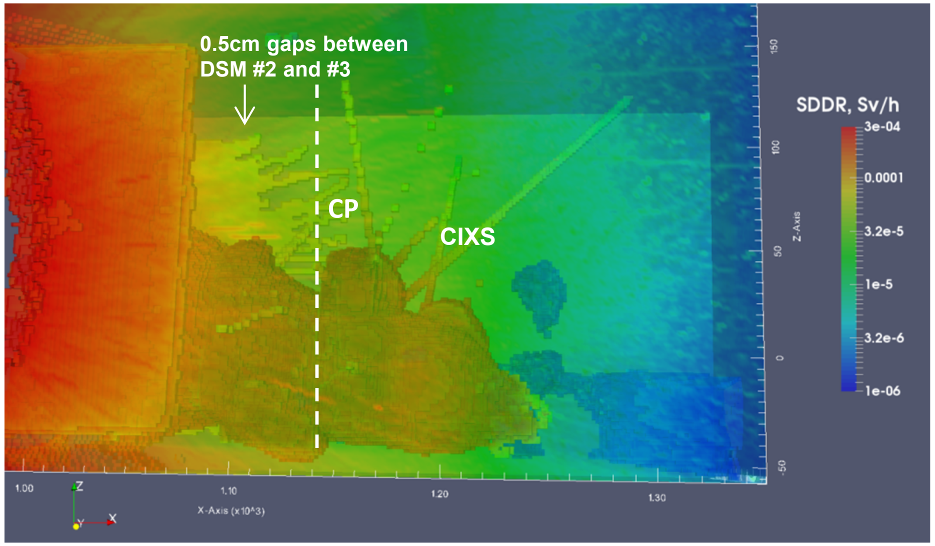

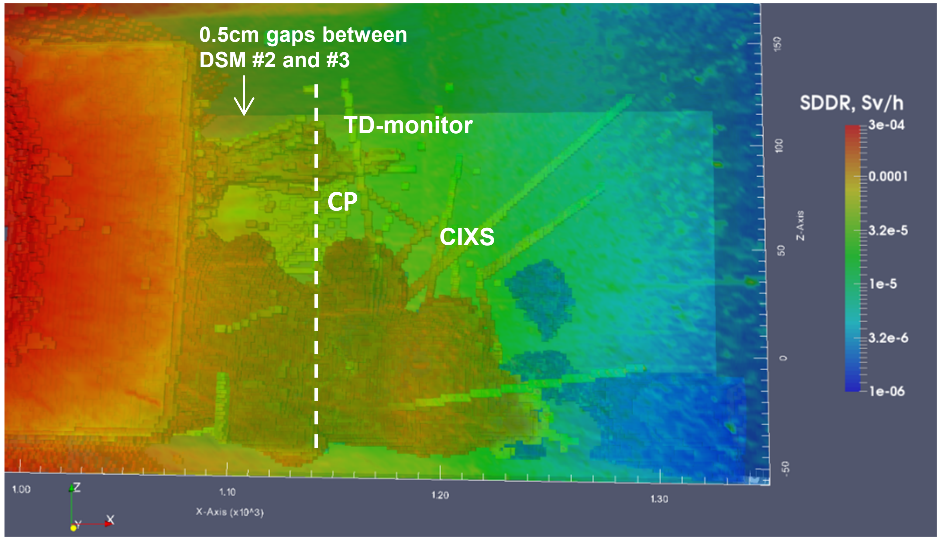

<u>Decay gamma streaming pathways</u>:

1) 0.5 cm gaps between DSM #2 and #3
2) CIXS

<u>Decay gamma streaming pathways</u>:

1) 0.5 cm gaps between DSM #2 and #3
2) CIXS
3) TD-monitor

SDDR comparison in spherical detectors in PI of EPP17

SDDR (microSv/h) distributions	CIXS-only model (with B4C shielding blocks around the vacuum flange), SDDR (microSv/h)	TD-monitor & CIXS model, SDDR (microSv/h)	Effect of TD-monitor on SDDR in spherical detectors: SDDR difference in models (T-mon & CIXS) – CIXS
	Layer #1 (L1):		
Vertical distribution at 30 cm from CP Left side- Layer #1 (L1)	Top side: 42	49	7
	56	64	8
	69	74	5
	66	68	2
	Bottom side: 76	78	2
	Layer #3 (L3):		
Vertical distribution at 100 cm from CP Left side (@ CIXS Crystal in Ex-Port box) - Layer #3 (L3)	Top side: 10	11	1
	8	9	1
	9	10	1
	17	17	0
	Bottom side: 30	33	3
Vertical distribution at 100 cm from CP Right side (@ Detector Ex-Port box) – Layer #3 (L3)	Top side: 32	33	1
	30	32	2
	25	26	1
	19	20	1
	Bottom side: 17	17	0

SDDR (microSv/h) in spherical detectors of the EPP17 MCNP model with both systems: TD-monitor & CIXS

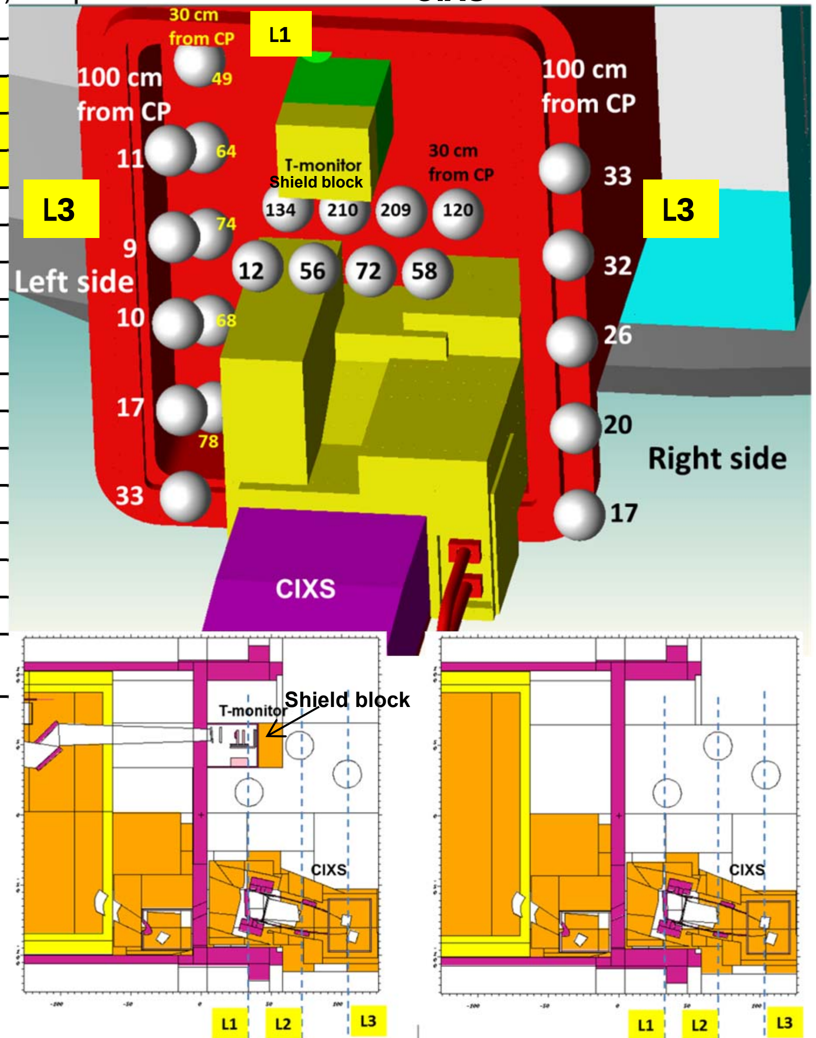

3 Layers (L1-L3) of spherical detectors were used for SDDR comparison in two MCNP models:

(1) SDDR in TD-monitor & CIXS model

(2) SDDR in CIXS-only model

Shield block (B4C) behind TD-monitor box was added to study its influence on SDDR in PI. It is compatible with the port plug remote handling, but this shield block has not been included in the structural integrity report.

SDDR horizontal distributions and effect of TD-monitor on SDDR

Horizontal SDDR (microSv/h) distributions in spherical detectors of TD-monitor & CIXS model

Layer #	Detectors location in horizontal distribution	Left			Right
L1	Below the TD-monitor, at 30cm from CP	134	210	209	120
L2	Behind the TD-monitor, at 66cm from CP	27	59	78	69
L3	Far from TD-monitor, 100cm from CP	12	56	72	58

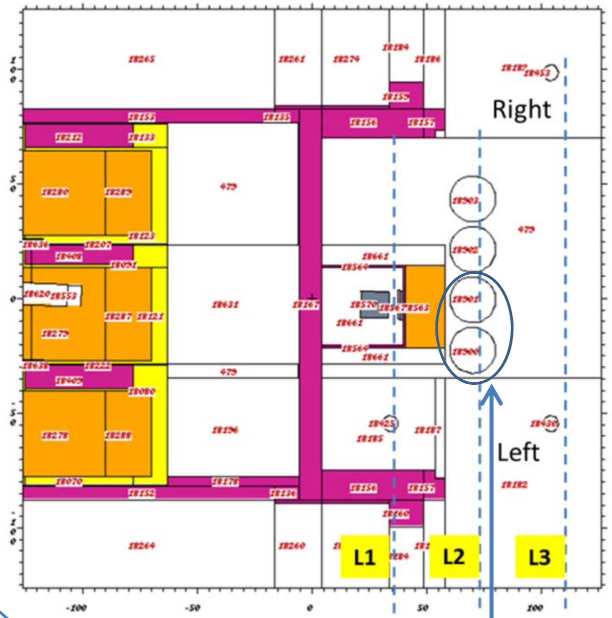

Horizontal SDDR (microSv/h) distributions in detectors of CIXS-only model

Layer #	Detectors location in horizontal distribution	Left			Right
L1	Below the TD-monitor, at 30cm from CP	121	193	194	117
L2	Behind the TD-monitor, at 66 cm from CP	32	66	74	63
L3	Far from TD-monitor, 100cm from CP	11	56	67	55

Gamma shadow effect for 2 detectors at L2 due to the shield of TD-mon box

Effect of TD-monitor on SDDR in spherical detectors. Difference of SDDR (microSv/h) in two models: (TD-mon & CIXS model) – CIXS-only model

Layer #	Detectors location in horizontal distribution	Left			Right
L1	Below the TD-monitor, at 30cm from CP	13	17	15	3
L2	Behind the TD-monitor, at 66cm from CP	-5	-7	4	6
L3	Far from TD-monitor, 100cm from CP	1	0	5	3

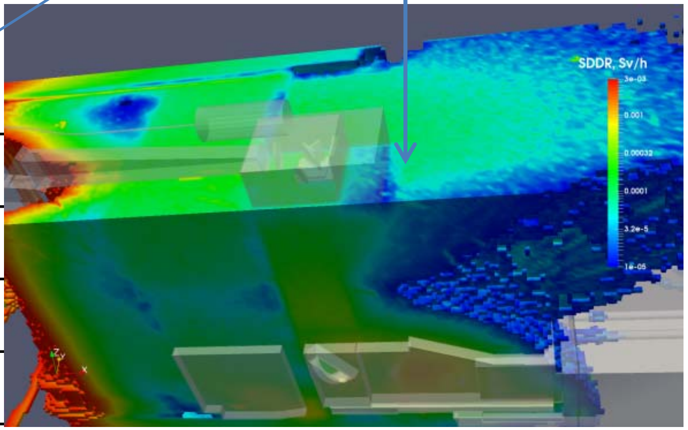

Summary and Recommendations

- Neutronics analysis was performed in the MCNP Local model of **EPP17** included only the apertures of two Diagnostics: TD-monitor and CIXS.
- The results include neutron and gamma fluxes and nuclear heating on **7 mirrors** of the TD-monitor, neutron fluxes and SDDR estimated in spherical detectors and with 3D distributions in EPP17:

  - Nuclear heating on mirrors is up to **0.77 W/cm^3 (**cooling might be required).
  - SDDR in spherical detectors at the bottom of TD-monitor shield box (at 30 cm from Closure Plate) reaches **210 microSv/h**, with a contribution of **17 microSv/h from TD-monitor.**
  - Shield block behind the TD-monitor contribute to a decrease on **7 microSv/h** – gamma shadow effect.
  - These are relative SDDR values of Local MCNP model. Final values request inclusion of all the tenants of EPP17 (TD-monitor, CIXS, Vis/IR system, and Divertor Thermography) – future task of EPP17 port plug integration, with inclusion of all the sorts of the gaps, radiation cross-talks between the ports, and environmental effects in global MCNP C-lite model.

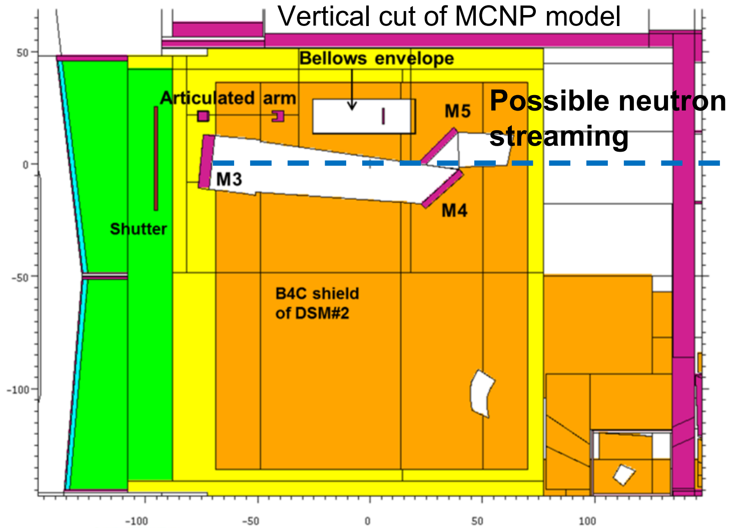

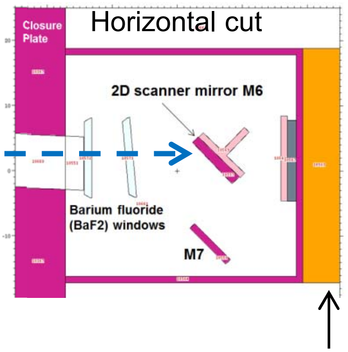

<u>Recommendations for TD-monitor design improvement:</u>

- Increase vertical shift (M4-M5) of the dog leg inside the port plug - to prevent possible direct neutron streaming.

- Shield block behind the TD-monitor optical box appears as a “neutronic relevant option”.

SDDR map in model with both systems: TD-monitor & CIXS

Gamma shadow effect due to the back-side shield of TD-monitor box in model with TD-monitor and CIXS

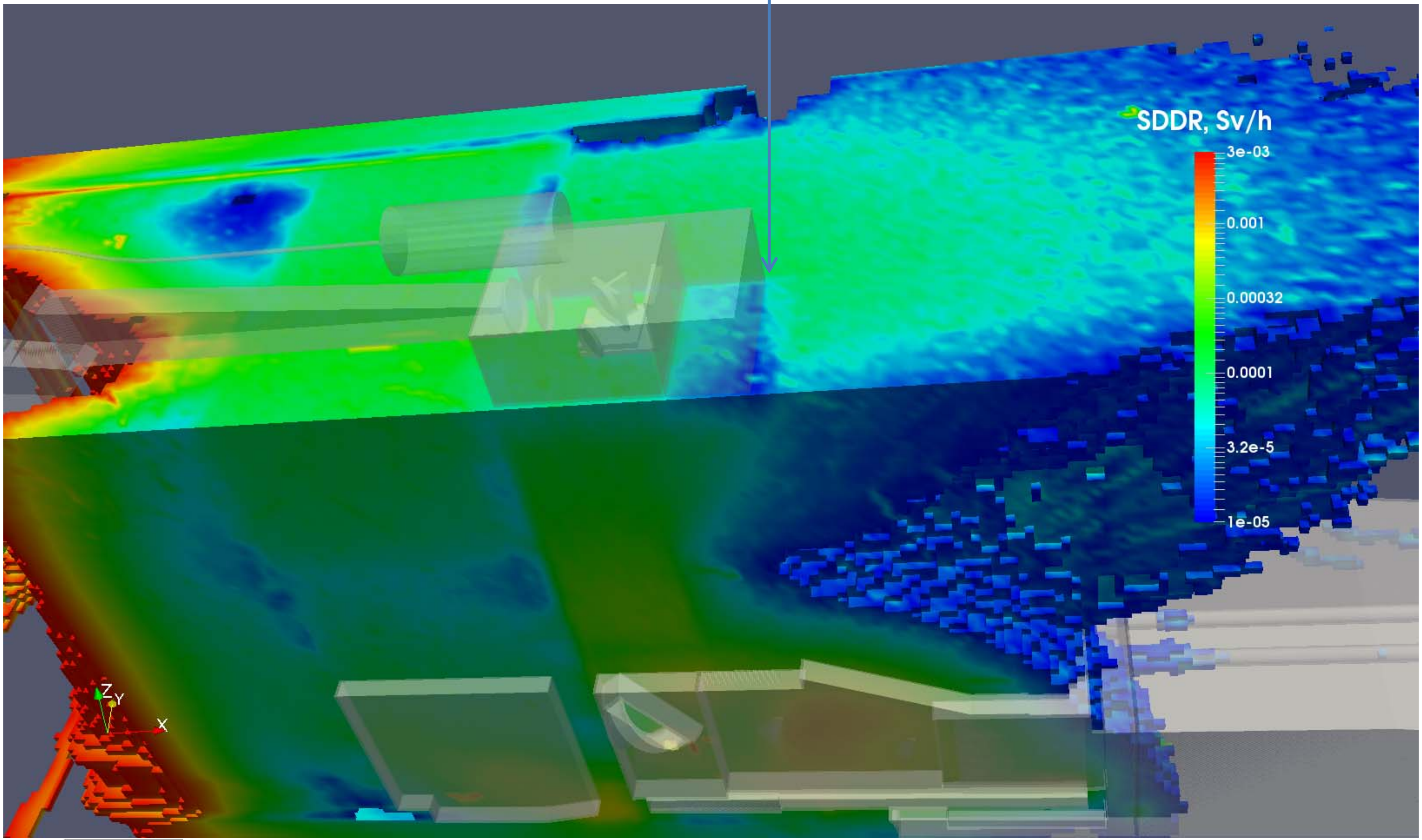

SDDR map in the EPP17 model with CIXS system only

No shadow observed in PI of the MCNP model included only the CIXS system

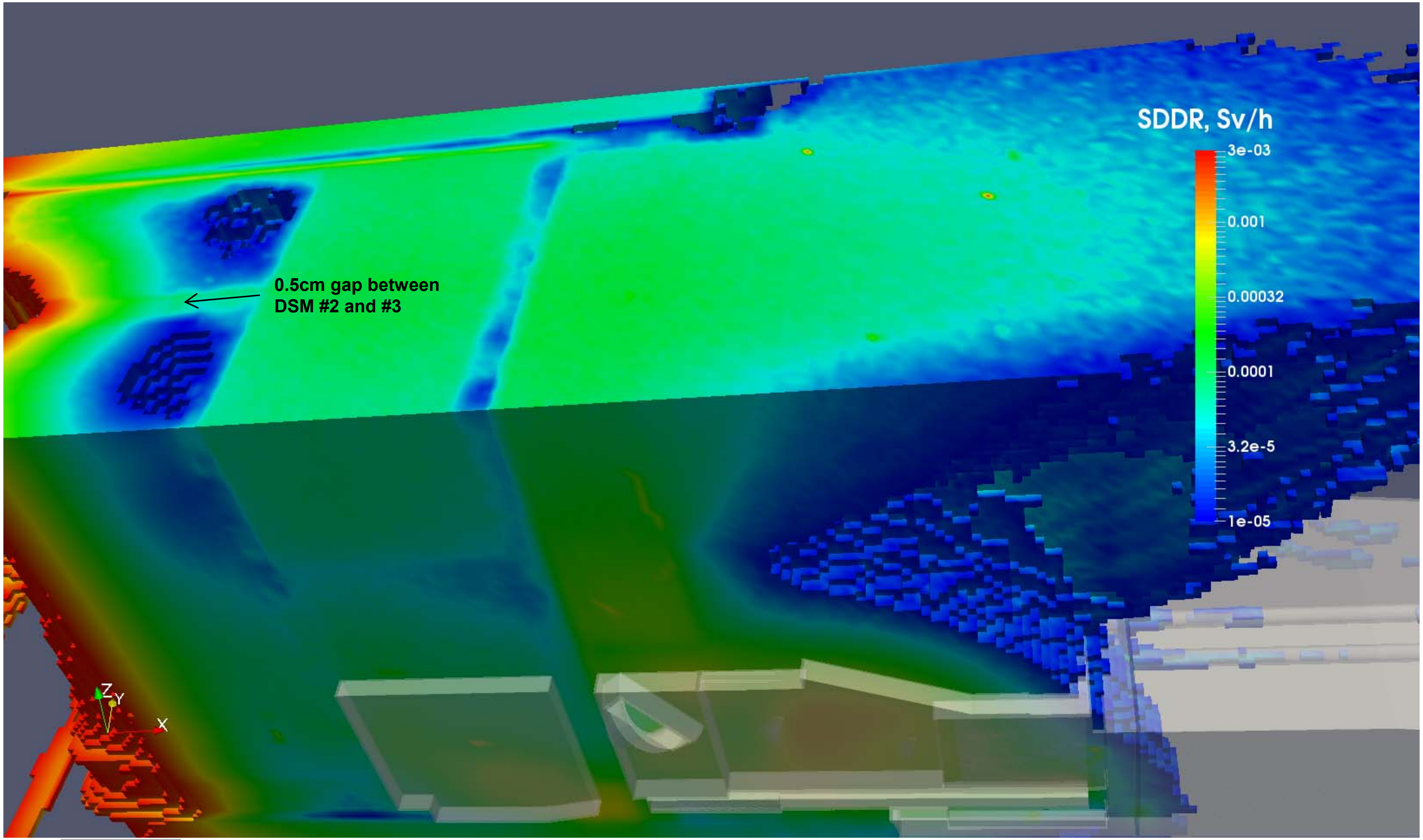

Gamma shadow effect due to the shield of TD-monitor box

Thresholded SDDR map (10 microSv/h – 100 microSv/h) to illustrate gamma shadow effect due to the back-side shield of TD-monitor box in model with TD-monitor and CIXS

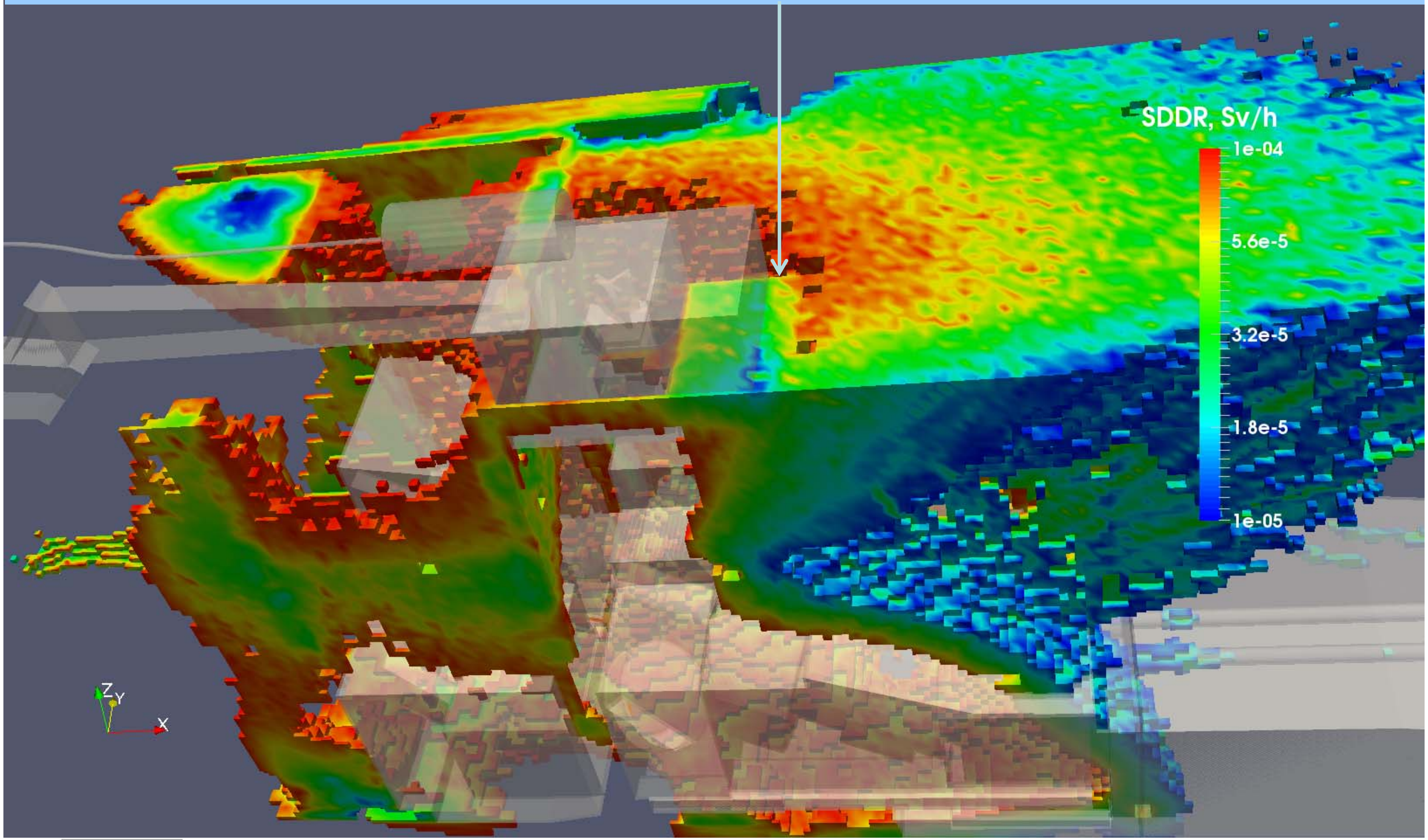

In-port radiation cross-talks

Example 2: Tangential Neutron Spectrometer (TNS) inside the **EPP #8** with 7 Diagnostics in C-lite v.2

Reduce (eliminate) radiation cross-talk from the Fast Ion Loss Detector (FILD) to Tangential Neutron Spectrometer (TNS) in EPP #8

Neutron spectra calculation in detectors of Tangential Neutron Spectrometer (TNS) inside the EPP8 with 7 diagnostic systems in C-lite v.2

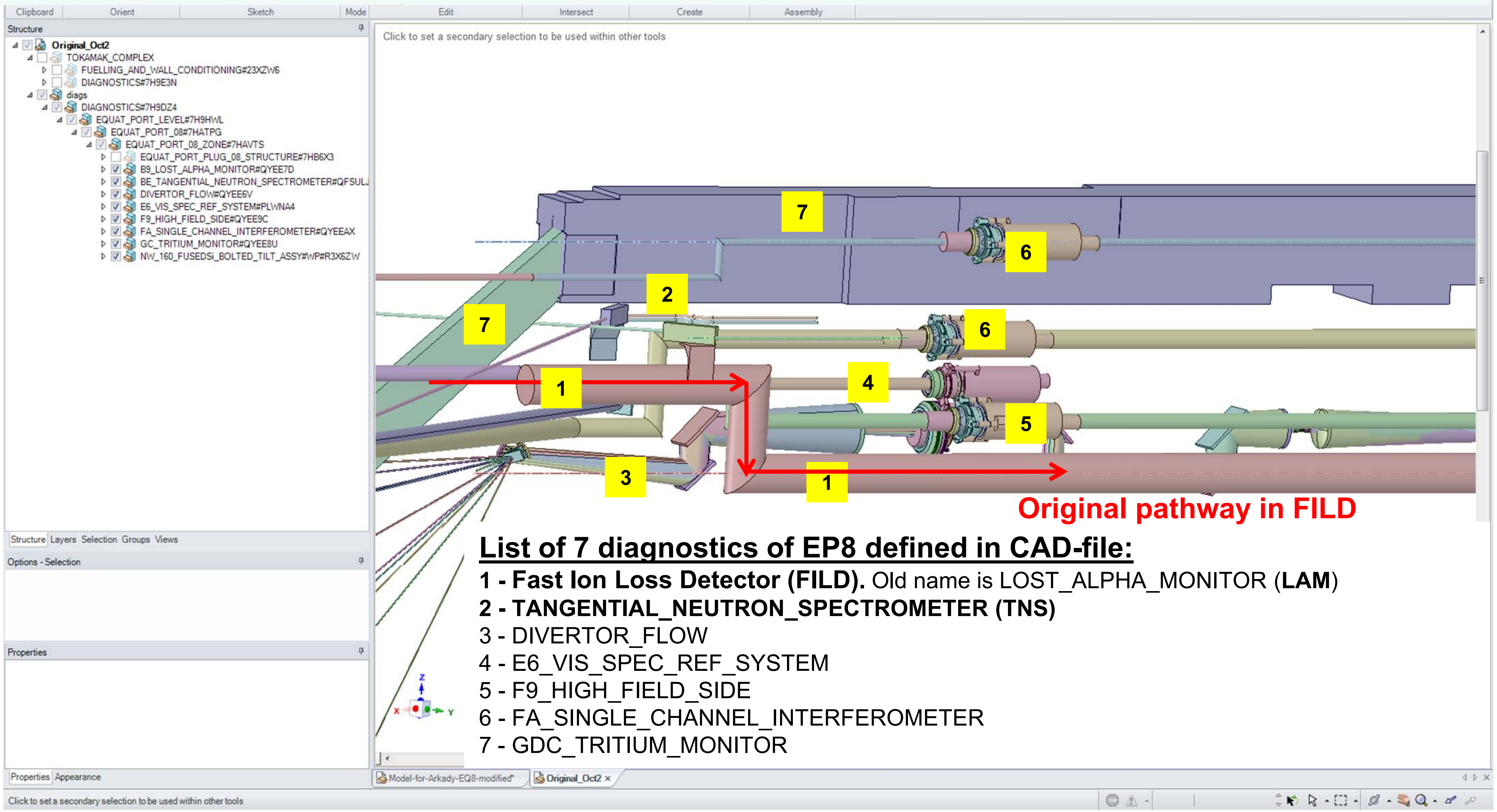

List of 7 diagnostics of EP8 defined in CAD-file:

1 - Fast Ion Loss Detector (FILD). Old name is LOST_ALPHA_MONITOR (**LAM**)
2 - TANGENTIAL_NEUTRON_SPECTROMETER (TNS)
3 - DIVERTOR_FLOW
4 - E6_VIS_SPEC_REF_SYSTEM
5 - F9_HIGH_FIELD_SIDE
6 - FA_SINGLE_CHANNEL_INTERFEROMETER
7 - GDC_TRITIUM_MONITOR

Filled LAM with the EQ8 shield material (B4C), numerical results are available:

https://user.iter.org/?uid=S36B22 with Excel file with neutron spectra in TNS of the EQ8 without Lost Alpha Monitor (S36B22)

Neutron streaming in FILD (LAM) path:

Peak factor (F_14MeV_per lethargy/F_sum E>10MeV)= 4.4705E+00	Ratio uncollided/total = 2.0488E-04

If FILD (LAM) is filled with shield - then peak factor is increased by two times (8.2), but ratio of uncollided flux to total flux is decreased by two times (1.08e-4). This is due to stronger moderation of neutrons by the shield:

Peak factor (F_14MeV_per lethargy/F_sum E>10Mev)= 8.1998E+00	Ratio uncollided/total = 1.0779E-04

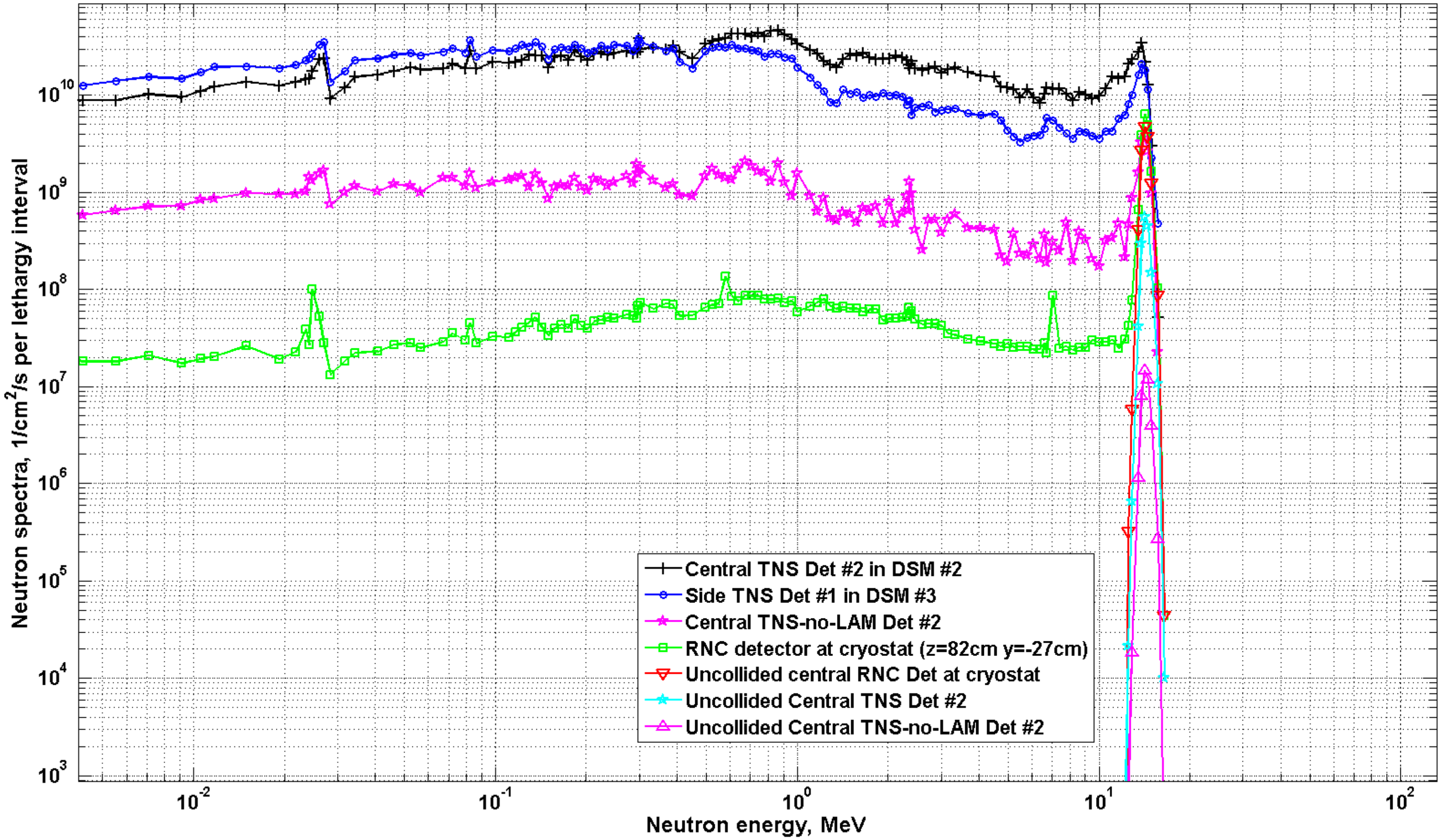

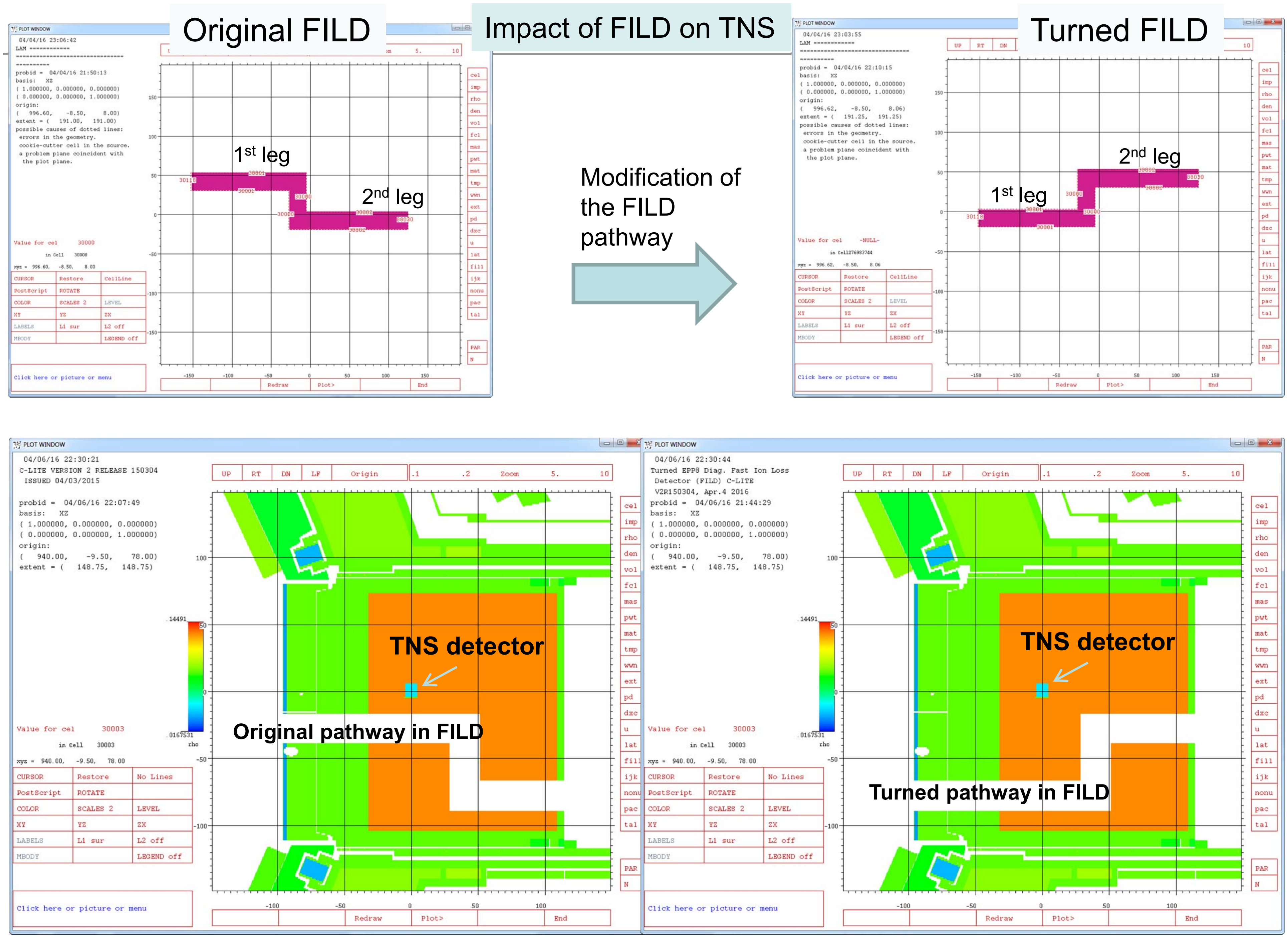

Impact of FILD on TNS
Original FILD
Turned FILD
1st leg
2nd leg
Modification of the FILD pathway
TNS detector
Original pathway in FILD
Turned pathway in FILD

MCNP neutron spectra calculations in TNS detectors of EPP #8 in C-lite V2 with turned upside-down LAM (FILD)

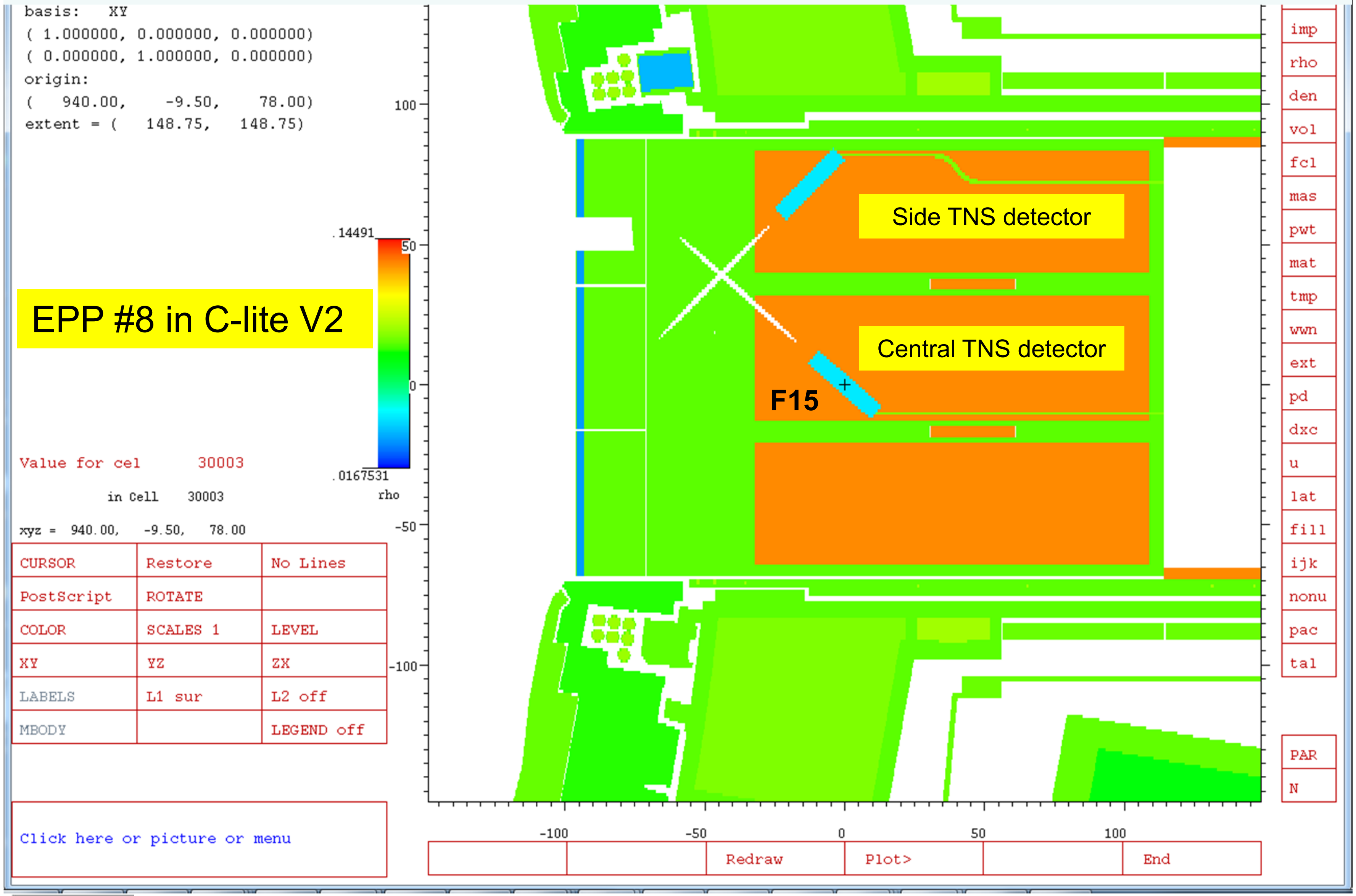

Original – vertical cross-cut

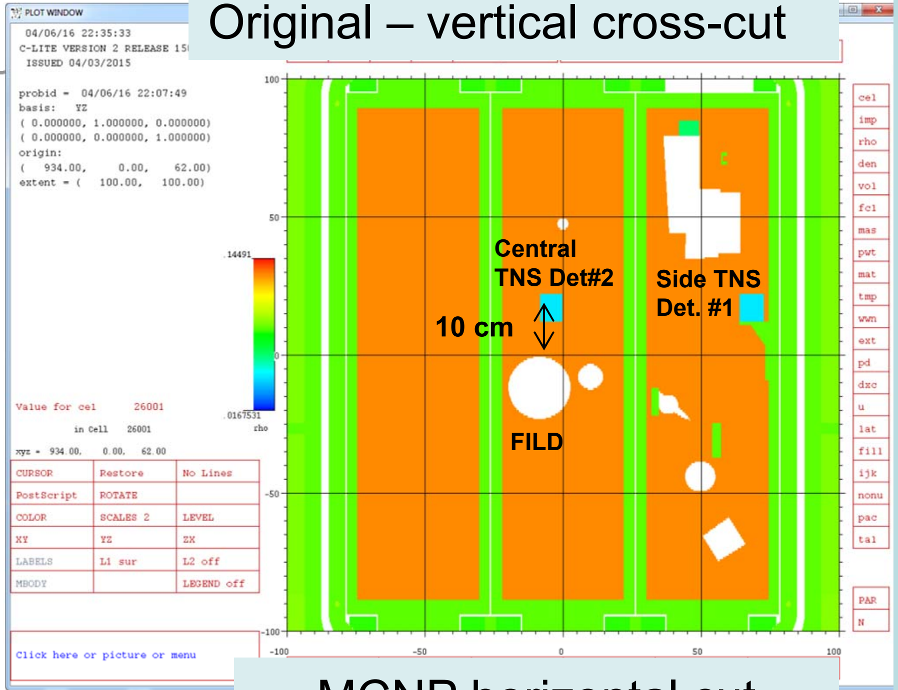

Turned - vertical cross-cut

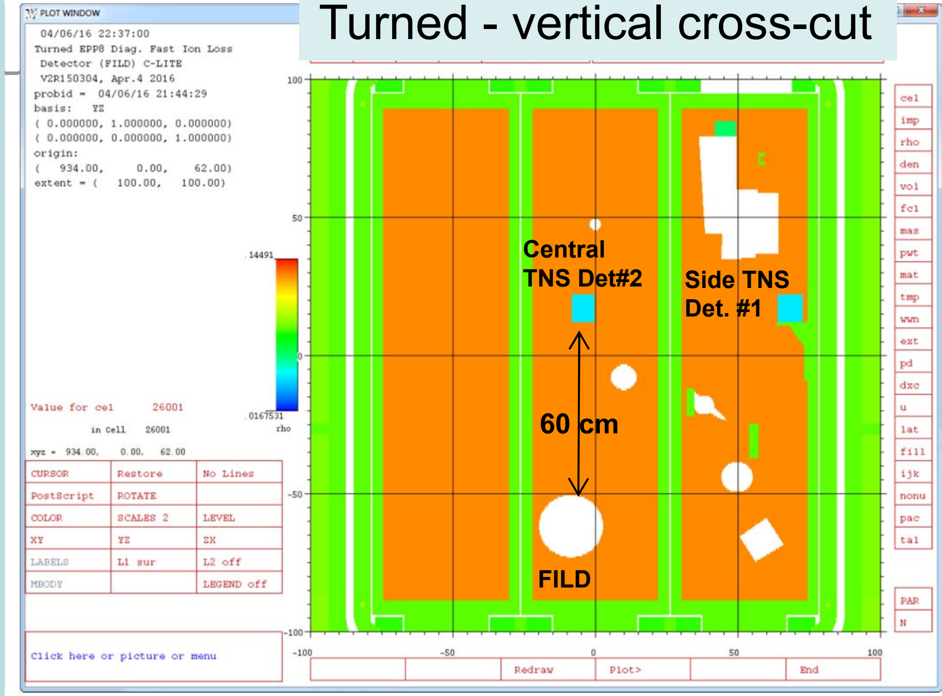

MCNP horizontal cut

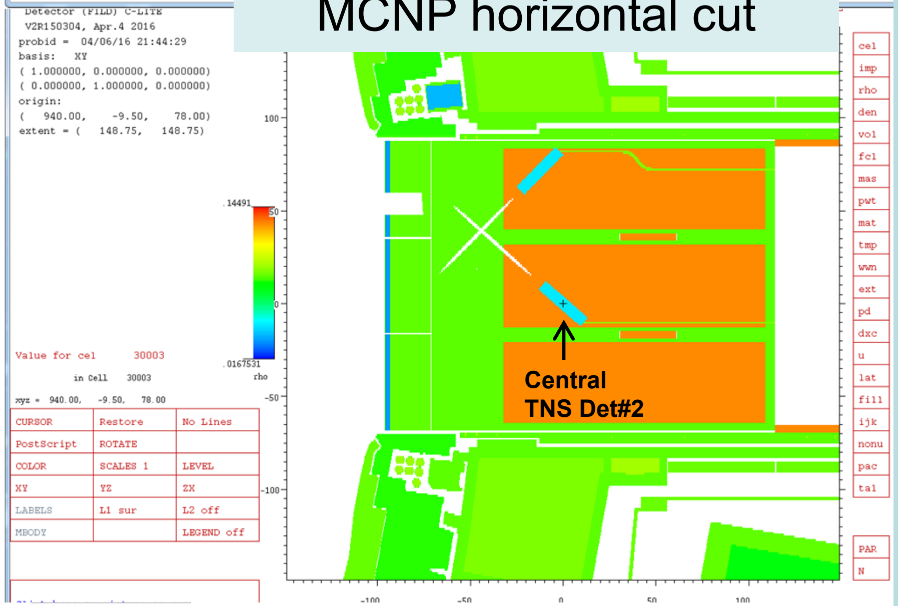

Investigation was carrying on for the Central TNS detector.
In the original EPP #8 model the distance between TNS and 1st leg of FILD was 10 cm, in the turned model it is 60 cm.

Turning upside-down of the FILD pathway helps to increase the 14-MeV peaking factor in energy resolution of the central TNS detector.

Turned FILD configuration stops neutron streaming from the FILD pathway to the Central TNS detector.

For measuring of n-spectrum in Central Det. #2 the turned FILD option is an equivalent to one of its absence – option of totally filled FILD (LAM – as FILD called before):
"TNS-no-LAM" case on the spectra plots next slide.

Eliminating cross-talks between TNS and LAM (FILD)

In Central TNS Detector #2 the neutron spectra are coincided for two cases:

1) Totally removed LAM (FILD)
2) Turned upside-down LAM (FILD)

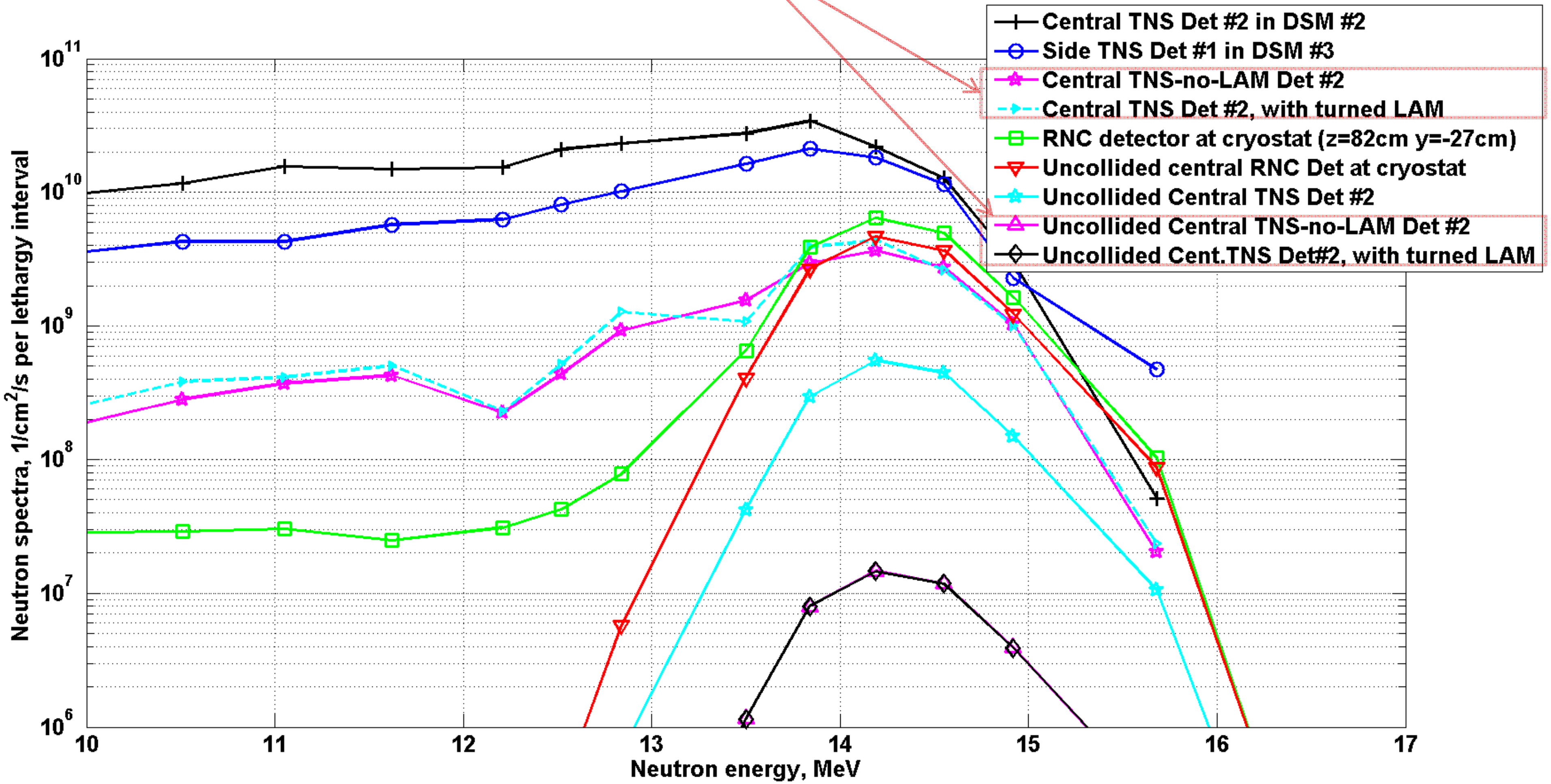

In-port radiation cross-talks

Example 3: Shutter and the main Diagnostic path of the Charge eXchange Recombination Spectroscopy (CXRS) in **UPP #3**

3 Cases of MCNP neutronic models considered in analysis of **C**harge e**X**change **R**ecombination **S**pectroscopy (**CXRS**) in UPP#3:

- **Case #1** of UPP#3 with CXRS and GDC;
- **Case #2** of UPP#3 with CXRS only;
- **Case #3** modified GUPP FDR 2013, with inclusion of single labyrinth in bottom gap

MCNP neutronic model

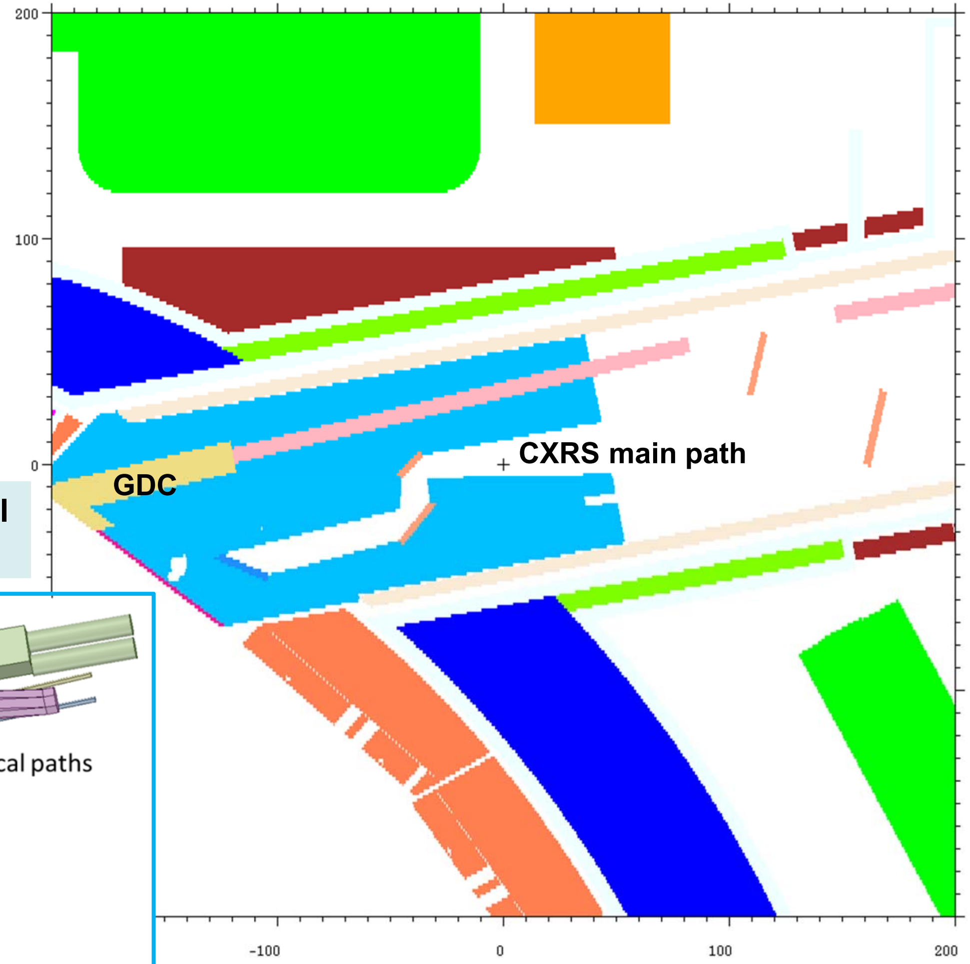

MCAM code used for CAD-to-MCNP model geometry conversion

CAD

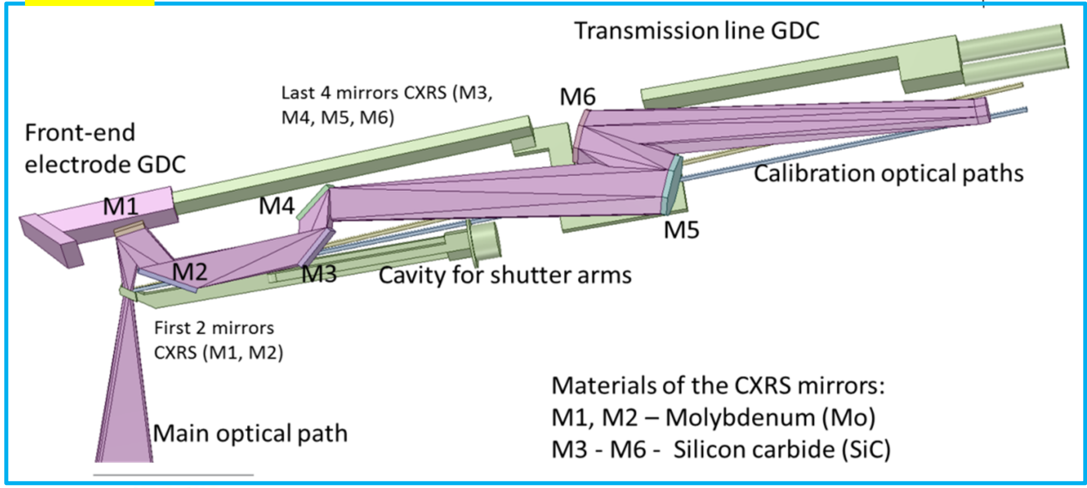

Detailed neutronics results for the CXRS mirrors

Materials of the CXRS mirrors:
M1, M2 – Molybdenum (Mo)
M3 - M6 - Silicon carbide (SiC)

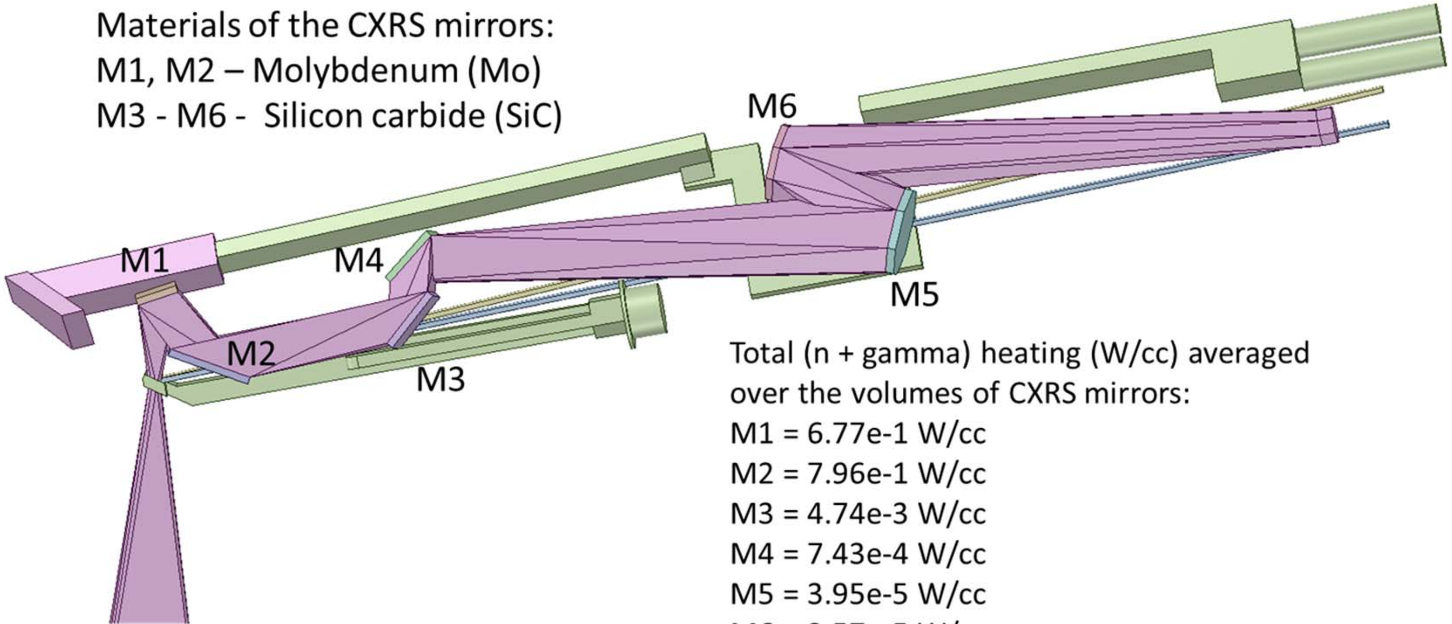

Total (n + gamma) heating (W/cc) averaged over the volumes of CXRS mirrors:
M1 = 6.77e-1 W/cc
M2 = 7.96e-1 W/cc
M3 = 4.74e-3 W/cc
M4 = 7.43e-4 W/cc
M5 = 3.95e-5 W/cc
M6 = 2.57e-5 W/cc

MCNP cell number	Mirror number	Material	Volume, cm3	Neutron flux, n/cm2/s	Gamma flux, gamma/ cm2/s	Neutron heating, W/cm3	Gamma heating, W/cm3	Total (n+gamma) heating, W/cm3
Cell 17500	M1	Molybdenum (Mo)	469.8000	2.50E+13	1.03E+13	1.48E-02	6.62E-01	6.77E-01
Cell 17512	M2	Molybdenum (Mo)	945.0000	3.04E+13	1.20E+13	1.79E-02	7.78E-01	7.96E-01
Cell 17502	M3	Silicon carbide (SiC)	907.5000	7.24E+11	2.89E+11	5.89E-04	4.15E-03	4.74E-03
Cell 17530	M4	Silicon carbide (SiC)	1061.1000	1.40E+11	5.03E+10	5.87E-05	6.84E-04	7.43E-04
Cell 17529	M5	Silicon carbide (SiC)	2748.0950	7.31E+09	2.91E+09	8.29E-06	3.13E-05	3.95E-05
Cell 17501	M6	Silicon carbide (SiC)	2150.2000	4.69E+09	1.47E+09	3.13E-06	2.26E-05	2.57E-05

For the interval of the MCNP statistical uncertainty (5%), the neutron and photon fluxes averaged for the 6 mirrors are the same for the UPP-CXRS with or without GDC.

Total neutron flux (n/cm2/s) mapped over **UPP with CXRS and GDC**

4 neutron streaming pathways in Case #1 of UPP-CXRS with GDC:

1 – Gaps all-round the UPP
2 – CXRS shutter
3 – CXRS main optical path
4 – GDC electrode

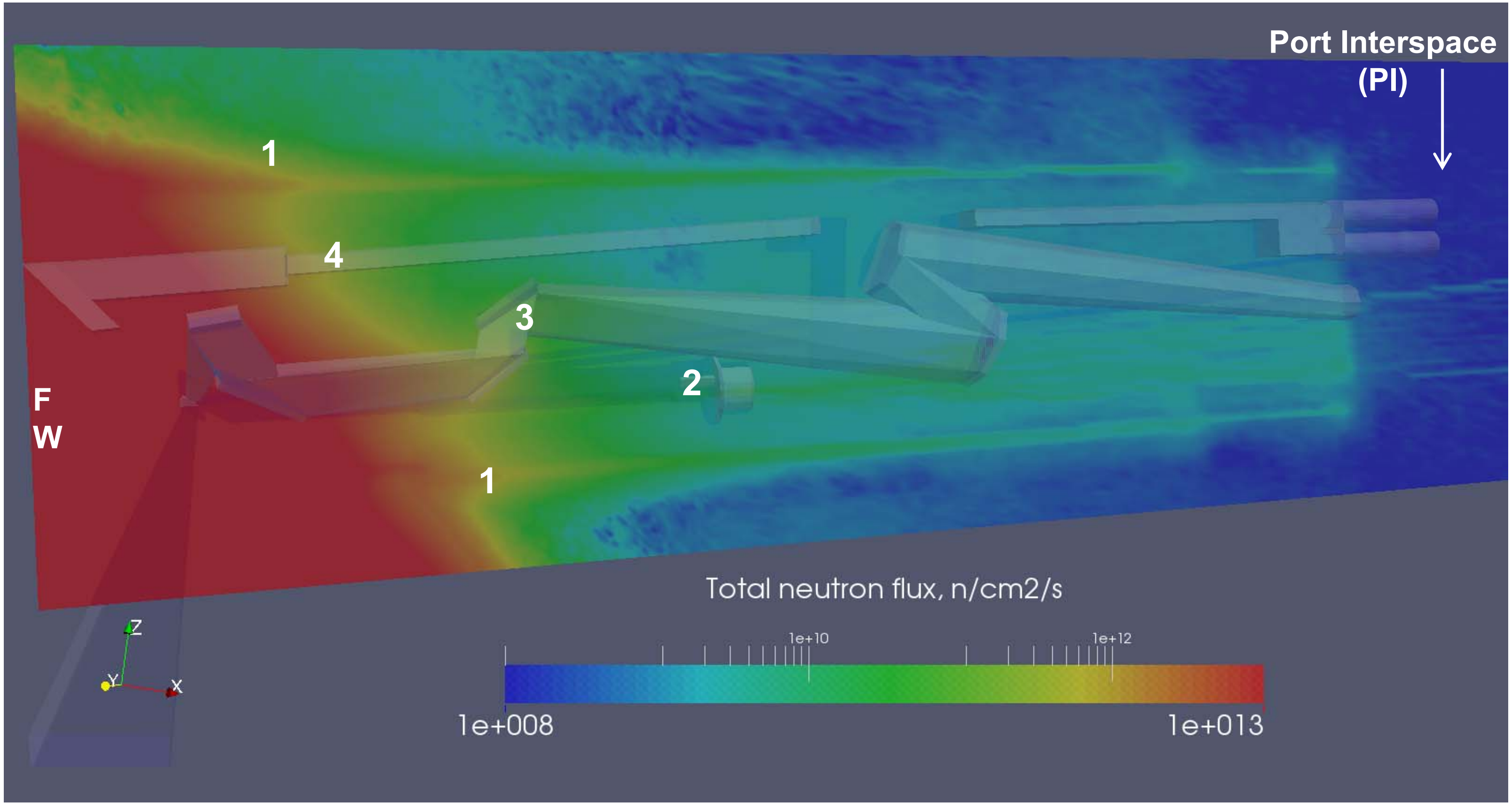

Impact of CXRS shutter – on neutron flux streaming

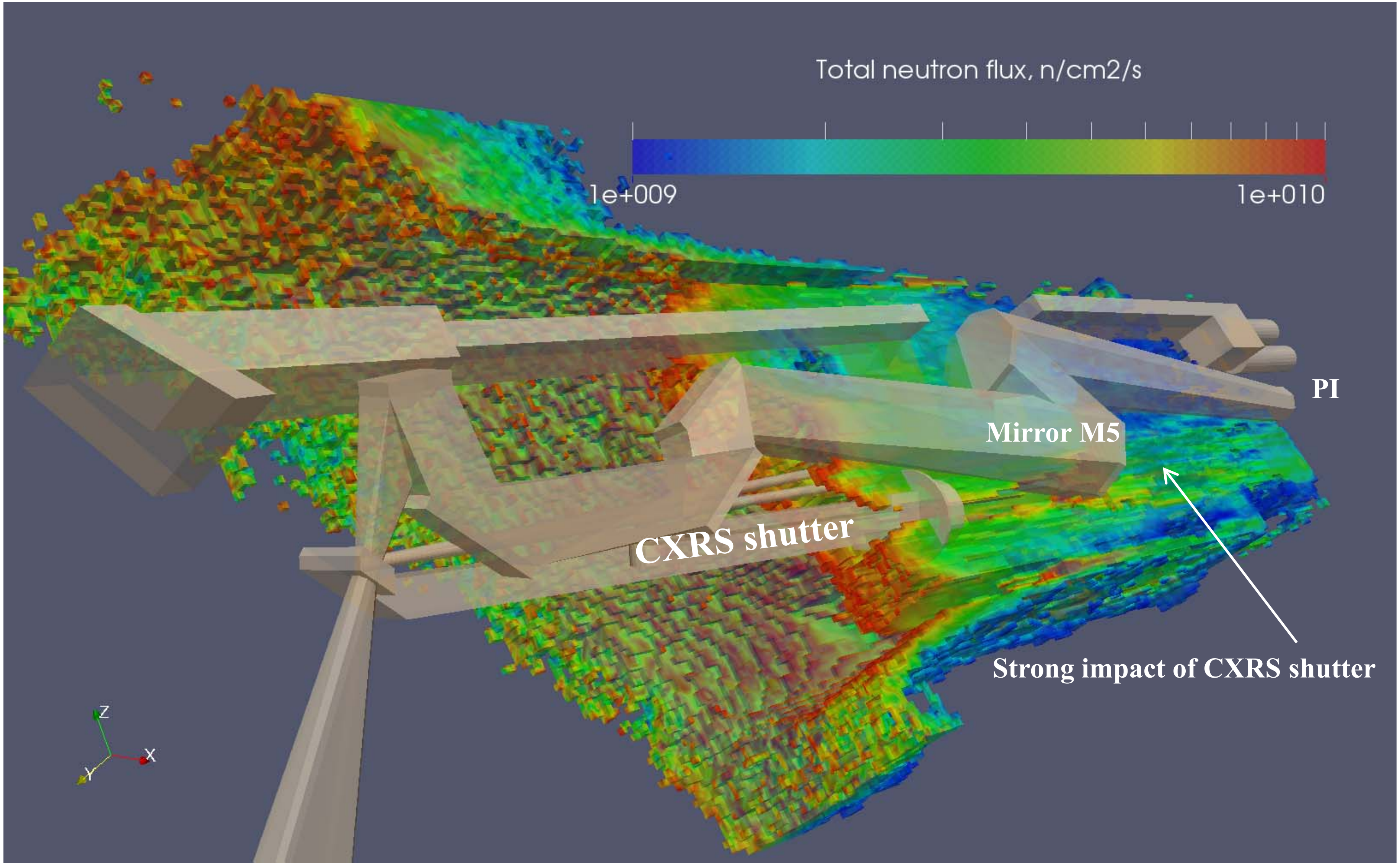

Case #1:
UPP-CXRS with GDC
4 pathways of neutron streaming :

1 – Gaps all-round the UPP
2 – CXRS shutter
3 – CXRS main optical path
4 – GDC electrode

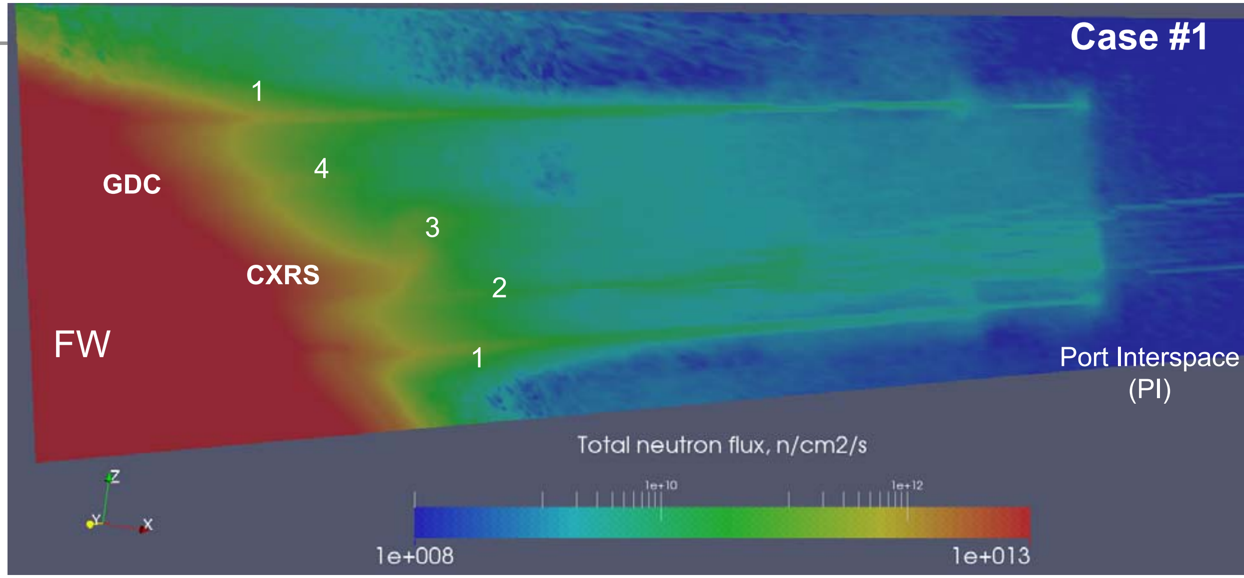

Neutron pathway analysis: Case #1 vs. Case #2:

Case #2:
UPP-CXRS except GDC
3 pathways of neutron streaming :

1 – Gaps all-round the UPP
2 – CXRS shutter
3 – CXRS main optical path

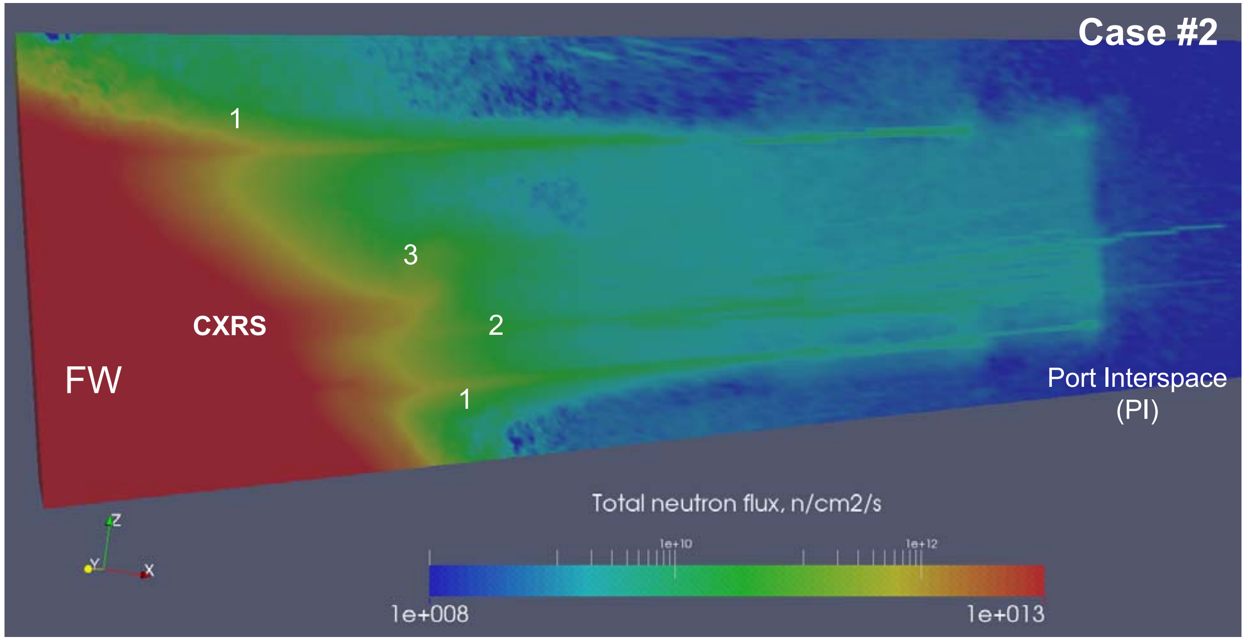

<u>Case 1</u>:
UPP-CXRS with GDC
4 pathways of neutron streaming :

- **1 – Gaps all-round the UPP**
- **2 – CXRS shutter**
- **3 – CXRS main optical path**
- **4 – GDC electrode**

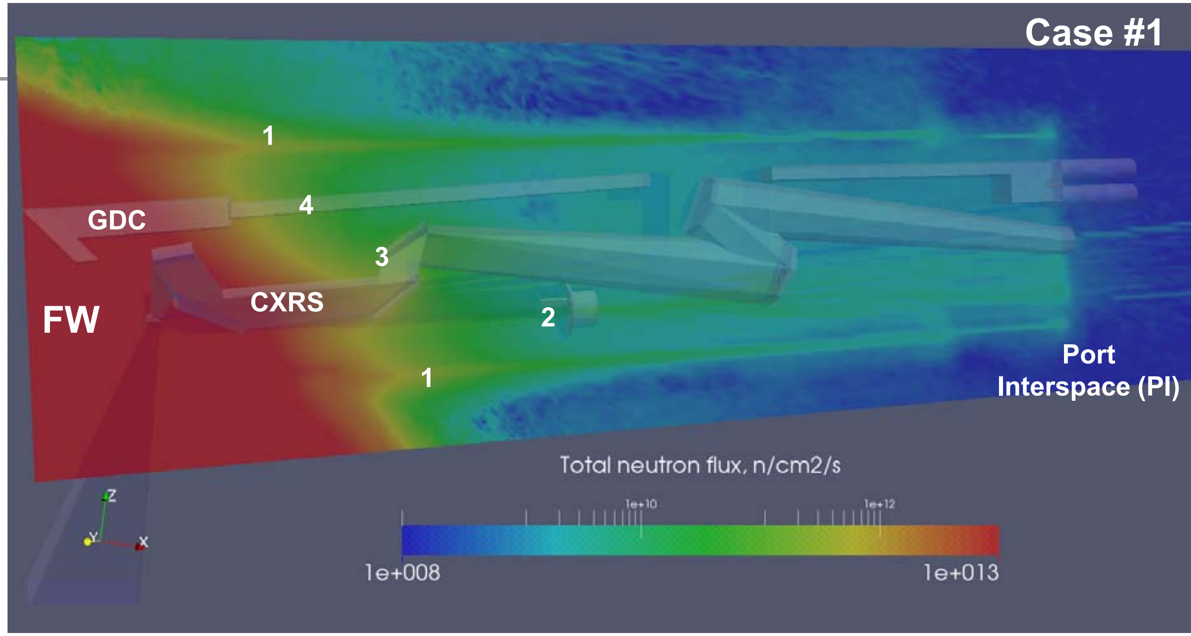

Neutron pathway analysis: Case #1 vs. Case #3:

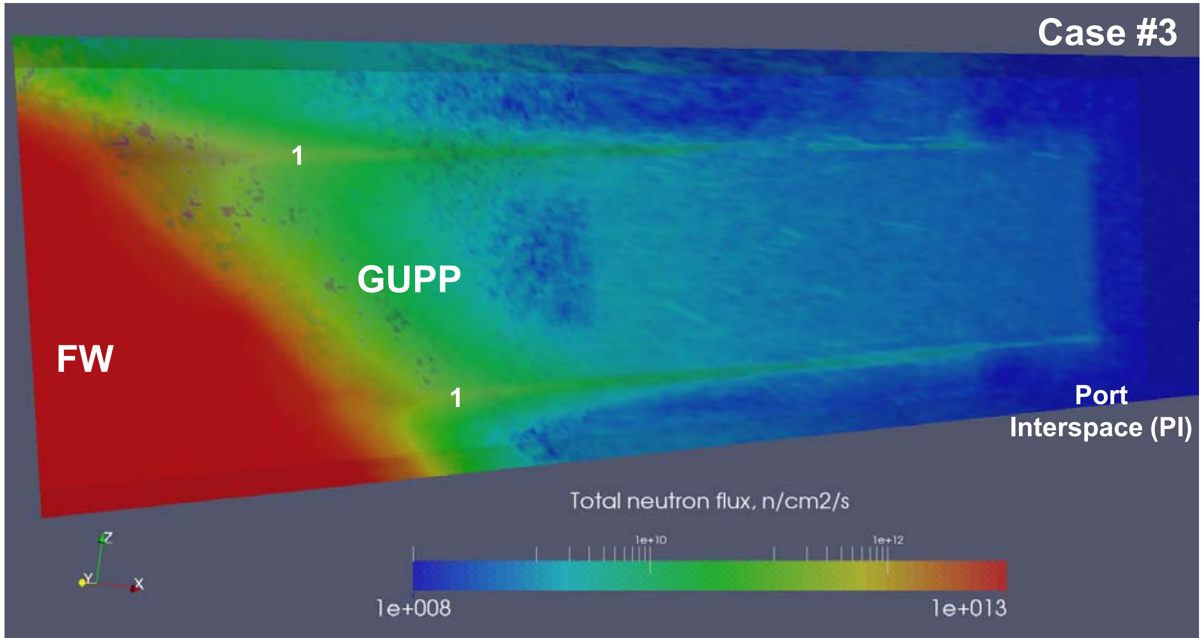

<u>Case 3</u>:
Generic UPP
1 pathway of neutron streaming :

- **1 – Gaps all-round the GUPP**

Total neutron & gamma fluxes inside Port Interspace (PI) volumes F3 & F4 for the 3 cases of UPP-CXRS

UPP interspace control volumes F3 & F4

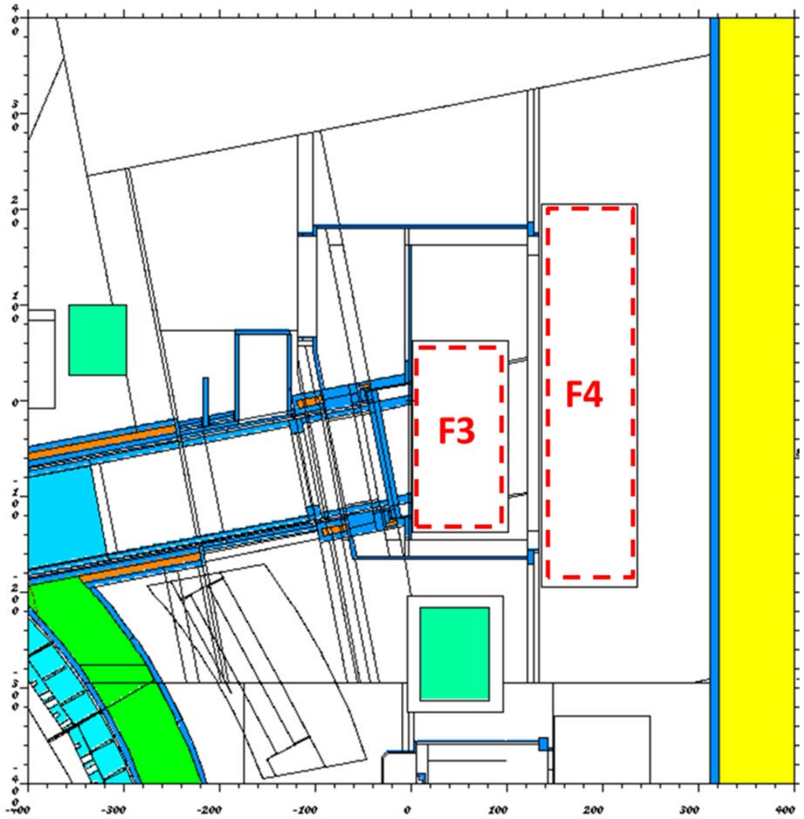

Case 1: UPP-CXRS with GDC	Neutron flux, n/cm2/s	Gamma flux, gamma/cm2/s
F3	9.48E+07	1.35E+07
F4	6.52E+07	9.42E+06

Case 2: UPP-CXRS except GDC	Neutron flux, n/cm2/s	Gamma flux, gamma/cm2/s
F3	9.65E+07	1.15E+07
F4	6.64E+07	8.64E+06

Case 3: Generic UPP	Neutron flux, n/cm2/s	Gamma flux, gamma/cm2/s
F3	7.61E+07	1.09E+07
F4	5.82E+07	8.54E+06

Conclusion: for the range of the MCNP statistical uncertainty (2%), neutron fluxes in Cases 1 & 2 are identical: in PI volume F3: **9.5e7 n/cm2/s**, in PI volume F4: **6.6e7 n/cm2/s**. For the Generic UPP with bulk shield plug, the neutron fluxes are lower: 7.6e7 n/cm2/s in F3, and 5.8e7 n/cm2/s in F4. That means the GDC system does not affect the SDDR in PI.

For the gamma fluxes the MCNP statistical uncertainty is higher – reaching 10%-15% of relative statistical error, where gamma fluxes are the following: 1.3e7 gamma/cm2/s in F3 and 9.0e6 gamma/cm2/s in F4.

SDDR results inside the PI-control volumes F3 & F4 for the 3 cases of UPP-CXRS configurations

Radioactive isotope	Case 1 of UPP-CXRS with GDC, microSv/h in F3	Case 1 of UPP-CXRS with GDC, microSv/h in F4	Case 2 of UPP-CXRS except GDC, microSv/h in F3	Case 2 of UPP-CXRS except GDC, microSv/h in F4	Case 3 of Generic UPP, microSv/h in F3	Case 3 of Generic UPP, microSv/h in F4
Cr 51	9.76E-01	6.96E-01	9.18E-01	6.70E-01	7.27E-01	6.00E-01
Mn 53						
Mn 54	4.76E+00	4.05E+00	3.53E+00	3.65E+00	2.01E+00	3.22E+00
Fe 55	1.44E+00	1.22E+00	1.21E+00	1.11E+00	6.45E-01	1.14E+00
Fe 59	3.76E+00	2.50E+00	3.67E+00	2.47E+00	3.28E+00	2.07E+00
Co 57						
Co 58	**1.79E+01**	**1.21E+01**	**2.09E+01**	**1.43E+01**	**1.44E+01**	**1.08E+01**
Co 60	**6.79E+01**	**5.23E+01**	**6.62E+01**	**5.19E+01**	**5.76E+01**	**4.90E+01**
Ni 58						
Ni 59						
Ni 63						
Zn 64						
Zr 93						
Nb 92						
Nb 92m						
Nb 93m						
Nb 94	7.84E-04	9.70E-04	7.54E-04	9.10E-04	7.81E-04	8.81E-04
Hf181						
Ta179						
Ta180m						
Ta182	**2.71E+01**	**1.80E+01**	**2.59E+01**	**1.78E+01**	**2.04E+01**	**1.43E+01**
Total dose	**1.24E+02**	**9.09E+01**	**1.22E+02**	**9.19E+01**	**9.90E+01**	**8.11E+01**

Conclusion: for the range of the statistical uncertainty (3%), the **SDDR results in Cases 1 & 2 are identical**: in PI volume **F3: 124 microSv/h**, in PI volume **F4: 92 microSv/h**. That means the GDC system does not affect the SDDR in PI. Comparison with the GUPP shows the contribution of CXRS system is **25 microSv/h in F3** and **10 microSv/h in F4**

Conclusions

- The phenomenon of in-port cross-talk was investigated for the diagnostic systems deployed in two Equatorial Port Plugs (EPP) #17 and #8, and for the components of Upper Port Plug (UPP) #3.
- The Core-Imaging X-ray Spectrometer (CIXS) inside the Diagnostic Generic EPP is analysed in EPP#17 local model, while EPP#8 is modelled globally with C-lite v2. The CXRS-GDC in UPP#3 was modelled using modified B-lite v.3 model.
- Multiple sets of diagnostic equipment inserted inside the same Port Plug create additional pathways for radiation streaming along the diagnostic channels and labyrinths (e.g. optical pathways) – the reason of in-port radiation cross-talk between different diagnostic systems.
- Demonstrated that in order to take advantage of particular shielding improvements in full extent, we should also assess the mutual influence of every Diagnostic system installed inside the same port.
- **This subject is important for Diagnostics designing at the stage of port integration to ensure engineering and maintenance solutions for the Diagnostic tenant systems.**